

AD-A124 689

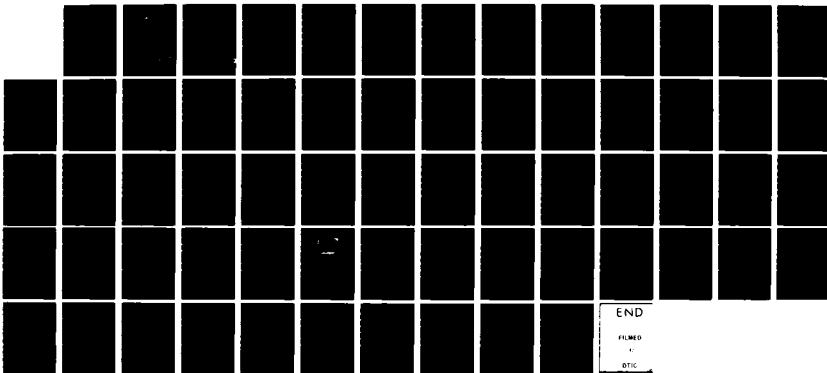
STUDY OF OHMIC CONTACTS ON Si(28) - IMPLANTED GAAS(U)
AIR FORCE INST OF TECH WRIGHT-PATTERSON AFB OH SCHOOL
OF ENGINEERING D M FISCHER DEC 82 AFIT/GEP/PH/82D-8

1/1

UNCLASSIFIED

F/G 20/12

NL

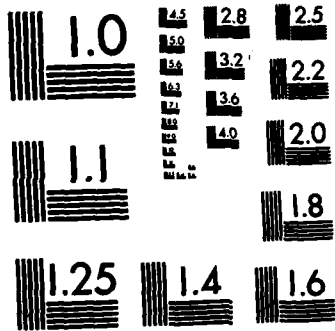


END

FILMED

11

DTIC

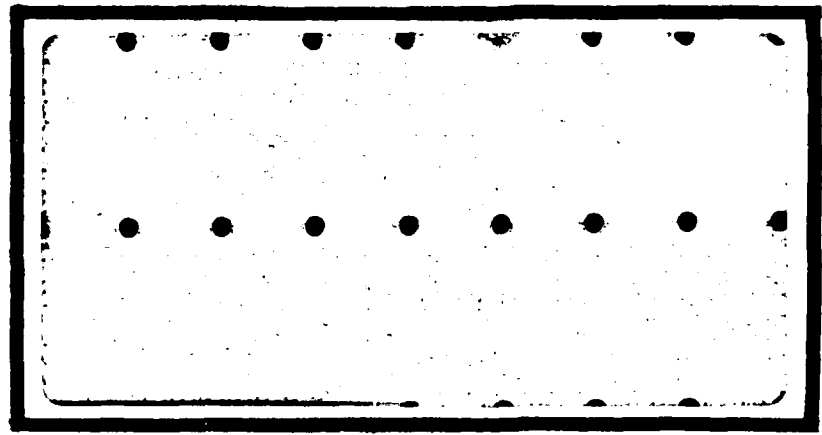


MICROCOPY RESOLUTION TEST CHART
NATIONAL BUREAU OF STANDARDS-1963-A

①



ADA 124689



This document has been approved
for public release and sale; its
distribution is unlimited.

S DTIC
ELECTE **D**
FEB 22 1983
A

DEPARTMENT OF THE AIR FORCE
AIR UNIVERSITY (ATC)

AIR FORCE INSTITUTE OF TECHNOLOGY

Wright-Patterson Air Force Base, Ohio

DTIC FILE COPY

02 10

AFIT/GEP/PH/82D-8

DTIC
COPY
INSPECTED
2

Accession For	
NTIS GRA&I	<input checked="" type="checkbox"/>
DTIC TAB	<input type="checkbox"/>
Unannounced	<input type="checkbox"/>
Justification	
Distribution/	
Availability Codes	
Avail and/or	
Dist	Special

A

STUDY OF OHMIC CONTACTS ON
Si²⁸- IMPLANTED GaAs
THESIS

AFIT/GEP/PH/82D-8

DIANE M. FISCHER
2LT USAF

DTIC
ELECTE
3 FEB 22 1983
A D

Approved for public release; distribution unlimited.

AFIT/GEP/PH/82D-8

STUDY OF OHMIC CONTACTS ON
 Si^{28} - IMPLANTED GaAs

THESIS

Presented to the Faculty of the School of Engineering
of the Air Force Institute of Technology

Air University

in Partial Fulfillment of the
Requirements for the Degree of
Master of Science

by

Diane M. Fischer, B.S.

2LT

USAF

Graduate Engineering Physics

December 1982

Approved for public release; distribution unlimited.

Preface

This thesis investigates the effect of contact fabrication on the specific contact resistivity. Different implantation doses of Si²⁸ at various annealing temperatures were tested for the lowest resistivity. This work limits its study to only AuGe/Ni contacts on GaAs. More extensive research needs to be conducted before any definite conclusions can be drawn. This work has developed a functional test procedure and indicated shortcomings in the contact pattern mask.

I would like to thank Dr. Y. K. Yeo for the time and effort which he spent discussing and aiding in this work. The insertion of a little positive psychology at appropriate times by Dr. Yeo helped me overcome the frustrations that are inherent in any experimental work. I am indebted to Dr. A. Ezis for his time and extreme patience. I also wish to thank Dr. Y. S. Park, Dr. R. Hengehold, and the Electronic Research Branch of the Wright Aeronautical Laboratories for sponsoring my work and supplying me with the necessary technical support.

Diane M. Fischer

Contents

Preface	ii
List of Tables	iv
List of Figures	v
List of Symbols	vi
Abstract	vii
I. Introduction	1
II. Theory	4
Ohmic Contacts and Resistivity	4
Mathematical Development	8
Determination of Specific Contact Resistivity	14
III. Test Equipment and Sample Preparation	15
Test Equipment	15
Sample Preparation	17
Ion Implantation	17
Sample Cleaning	17
Pyrolytic Encapsulation	18
Annealing	18
Removal of Si ₃ N ₄ Cap	18
Mesa Etching	19
Deposition of AuGe/Ni	20
Alloying	21
IV. Procedure	24
Measurements	26
Calculations	29
Error Bars	30
V. Results	33
Discrepancy Between Patterns	33
Negative y-intercept	35
Findings	36
Fixed Implantation Dose	36
Fixed Annealing Temperature	41
VI. Recommendations/Conclusions	46
Bibliography	51

List of Tables

Table		Page
I	Summary of Annealing Temperatures and Doses of Prepared Samples	19
II	Data Summary - Fixed Annealing Temperature .	42

List of Figures

Figure		Page
1	Band Diagram of a MS Contact on a Moderately Doped Semiconductor	5
2	Transfer Length Test Pattern	9
3	Schematic of Test Equipment	16
4	Illustration of Finished Sample with Contacts	23
5	Test Patterns Used to Evaluate Specific Contact Resistivity	25
6	Probe Positions on Test Patterns	28
7	Expected Graphical Results	31
8	Misalignment of Metal Contacts and Mesa	37
9	Resistance Versus Distance Plots of Experimental Data	38
10	Plot of ρ_c vs Annealing Temperature	39
11	Plot of R_{SH} vs Annealing Temperature	40
12	Plot of R_{SH} vs Dose	43
13	Plot of ρ_c vs Dose	44
14	Proposed Ohmic Contact Test Pattern	48

List of Symbols

E_F	- Fermi Energy Level
ϕ_B	- Potential Barrier Height
ϕ_m	- Metal Work Function
ϕ_s	- Semiconductor Work Function
W	- Space Charge Region
X_S	- Electron Affinity
I	- Current (amp)
J	- Current Density (amp/cm^2)
L_T	- Transfer Length (cm)
l	- Spacing Between Contacts (cm)
m	- Slope (Ω/cm)
ρ_C	- Specific Contact Resistivity ($\Omega\text{-cm}^2$)
R	- Resistance (Ω)
R_C	- Contact Resistance (Ω)
R_{SH}	- Sheet Resistance (Ω/\square)
S_x	- Standard Deviation
t	- Degree of Certainty for a Given Degree of Freedom
μ	- Predicted Range
\bar{x}	- A Mean Value
x	- Length (cm)
x_C	- Contact Length (cm)
x_{L_T}	- Apparent Transfer Length (cm)
z	- Contact Width (cm)

10 to the 13th power

15 to the 15th power

Abstract

A study of fabricating a low resistant contact on Si⁽²⁸⁾-implanted n-type GaAs was conducted. Ion doses of $1 \times 10^{13} / \text{cm}^2$ to $1 \times 10^{15} / \text{cm}^2$ and annealing temperatures of 700°C to 900°C were tested in order to achieve the lowest specific contact resistivity. Experimental results show that a low specific contact resistivity of $2.78 \times 10^{-7} \Omega/\text{cm}^2$ can be obtained on GaAs layers which have been formed by Si⁽²⁸⁾ ($3 \times 10^{14} / \text{cm}^2$) implantation in undoped semi-insulating GaAs annealed at 850°C using an oxygen-free chemical vapor deposited Si₃N₄ layer as an encapsulant followed by subsequent deposition of AuGe/Ni ohmic contacts. Recommendations are discussed concerning further studies and a design for a new contact test pattern which would improve the degree of accuracy of resistivity measurements.

ohm

10 to the 14th power

10 to the 15th power

STUDY OF OHMIC CONTACTS ON

Si²⁸ - IMPLANTED GaAs

I Introduction

In the world of high speed electronic device applications, interest has developed in producing devices using gallium arsenide (GaAs). The problem lies in fabricating a good reliable low-resistance contact to such devices. An ideal ohmic contact allows current flow in either direction without any resistance, however such an ideal contact is not always possible to produce in a working environment. A potential barrier between metal and semiconductor interface is nearly always present to make the contact less than ideal (Ref 1). A contact may still be considered ohmic if the resistance is small and the voltage drop is linear with the changes in the current flow. Numerous studies have been made on minimizing the effect of the barrier and reducing the contact resistance (Ref 2, 3, 4, 5).

The ohmicity of a contact is often evaluated in terms of its specific contact resistivity, ρ_c (Ref 5, 6, 7); the units of ρ_c being in $\Omega\text{-cm}^2$. Ideally, $\rho_c = 0$, but normally ρ_c is not zero. A low-resistance ohmic contact has a ρ_c of typically $\sim 10^{-6}\Omega\text{-cm}^2$, however even lower resistances are desired.

Research on the theory of metal-semiconductor interfaces and their current transport characteristics are usually considered to have begun with work of Mott (Ref 8) and Schottky (Ref 9). The initial experimental work on developing alloyed typed ohmic contacts to GaAs was performed by Cox and Strack (Ref 10). Since that time, various methods for fabricating ohmic contacts have been examined. The usual technique alloys a Au-Ge contact mixture into the GaAs surface. The Ge is believed to move into the GaAs surface and creates a highly doped region which forms a thin space charge layer that electrons can tunnel through. Usually thermal alloying is performed, but laser annealing and electron beam annealing (Ref 11) has gained current interest. As a means to reduce the contact resistance, ion implantation has been tried with success (Ref 3, 4, 12). Various ion species have been studied such as Si, Se and (Se+Ge) that have produced contacts with reported resistivities of $\sim 3 \times 10^{-7} \Omega\text{-cm}^2$ (Ref 3).

More importantly, a dependable means of fabricating a low-resistance contact needs to be developed since so often an ohmic contact is fabricated but then cannot be reproduced (Ref 5, 13). One objective of this work is to obtain predictable results from a fabrication process in particular, the process of ion implantation. As a second objective, this research sought to minimize ρ_c by varying implantation doses and the annealing temperatures. The implantation of

ions serves to increase the number of carriers in the material and therefore to reduce the contact resistance. The annealing process activates the implanted ions by placing the ions in lattice sites within the crystal structure.

This thesis presents a brief background on the theory surrounding ohmic contacts and resistivity along with a mathematical development in Section II. Section III gives a description of the equipment used in the research; plus the procedure for preparing the sample, taking the measurements, and performing the calculations. The data and results are presented in Section IV. This paper concludes with recommendations for further studies in Section V.

II Theory

Before any discussion of contact performance and ohmic contacts, one must have a clear meaning of the word "ohmic". To define this term, the structure of the metal-semiconductor (MS) interface has to be considered. The nature of ohmic contacts and specific contact resistivity will be discussed in this section. Finally, a mathematical approach that leads to solving for the contact resistivity will be presented.

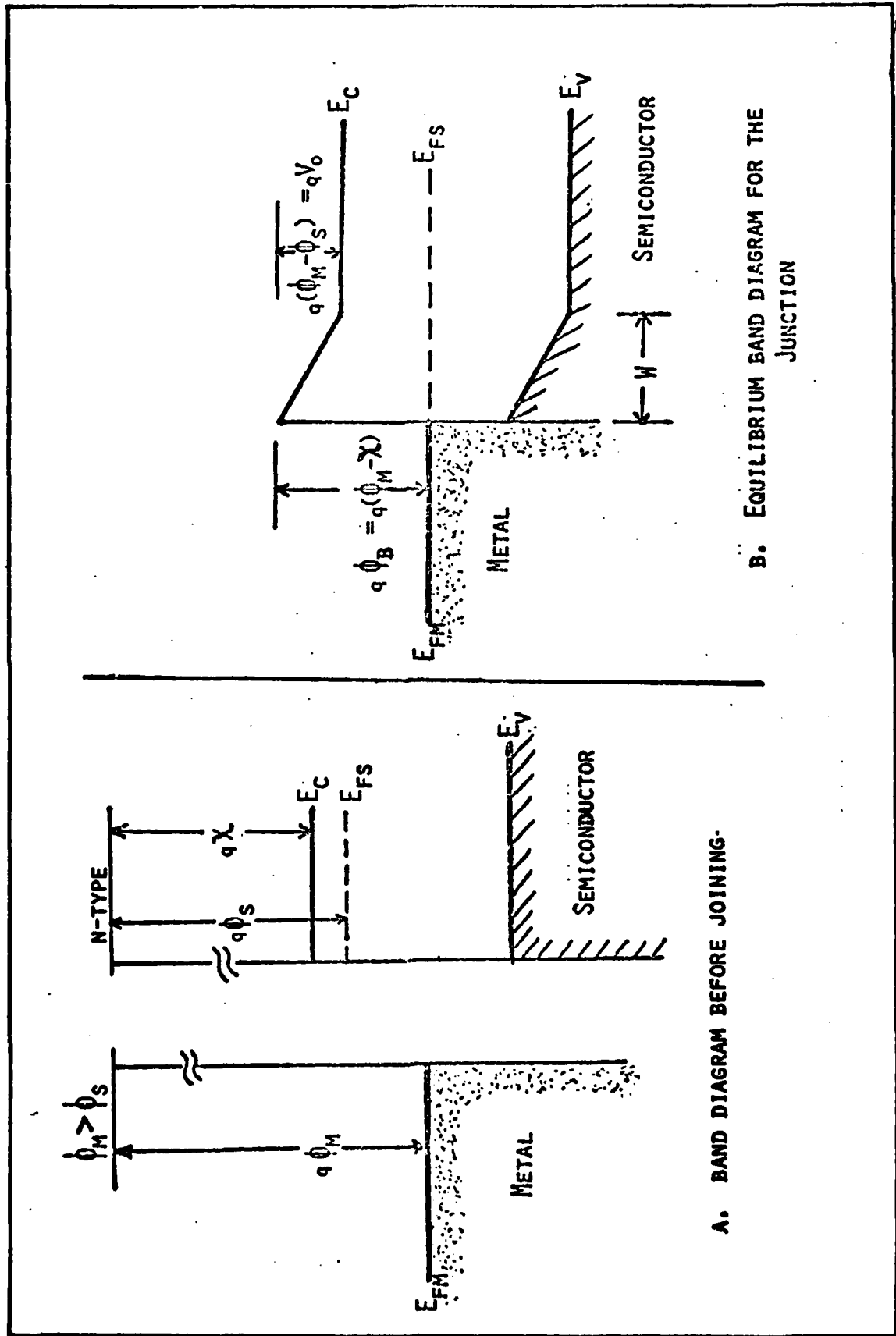
Ohmic Contacts and Resistivity

When a metal and semiconductor are joined, a potential barrier is formed at the interface. Figure 1 shows the band diagram of a MS contact on a moderately doped semiconductor. This type of barrier is referred to as a Schottky barrier. In the figure, E_c and E_v represent the semiconductor conduction and valence bands, respectively. The Fermi energy level is E_F . The potential barrier height is given by ϕ_B and the space charge region width is W .

Classically ϕ_B is defined as

$$\phi_B = \phi_m - X_s$$

where ϕ_m is the metal work function and X_s is the electron affinity of the semiconductor (Ref 14). If $\phi_m > \phi_s$, where ϕ_s is the semiconductor work function, the barrier of



A. BAND DIAGRAM BEFORE JOINING.

B. EQUILIBRIUM BAND DIAGRAM FOR THE JUNCTION

Figure 1. Band Diagram of a MS Contact on a Moderately Doped Semiconductor

Figure 1 results. This barrier impedes the current flow and even for low values of current, large voltage drops appear across this interface which can result in a large contact resistance.

If $\phi_m < \phi_s$, ϕ_B can become zero or even negative. In such a case, the current sees essentially no resistance since no barrier exists. An ideal contact is defined as one that has zero contact resistance. The most desirable contacts are ohmic contacts with zero contact resistance. However, most practical MS combinations do produce a barrier and therefore a less than ideal contact. Obviously when fabricating ohmic contacts onto devices, the goal is to have a smaller voltage drop across the contact interface than the voltage drop across the bulk region of the device. This minimizes the presence of the contact so that the contact does not affect the performance of the device. The I-V response of the contact should be linear as well. In this case, the description of "ohmic" becomes a relative one, being compared to the bulk resistance of the device.

A more quantitative way to describe ohmic contact performance is in terms of specific contact resistivity, ρ_c , which is given in units of $\Omega\text{-cm}^2$. The definition of ρ_c lumps together the effects of the contact interface into a single distributed resistance. If the I-V response of the interface is linear, the value of ρ_c is applicable over all voltage drops. If the I-V response is non-linear, then the

ρ_c value is applicable only at one particular value of I and V. Lower values of ρ_c are preferred.

When contact current flow is perpendicular to the interface, the resistance of a contact of a given area A can be stated as

$$R_c = \frac{\rho_c}{A} \quad (1)$$

and voltage drop across the contact is calculated from

$$V_c = IR_c \quad (2)$$

For current flow in a planar contact, current flow is not strictly perpendicular therefore Eq. (2) cannot be applied directly. A different method must be used to relate V_c to I and ρ_c (Ref 6, 7). In such cases, the concept of ρ_c is still a valid and convenient way to characterize the performance of the contact. Therefore a contact with sufficiently small ρ_c values could be called "ohmic". Normally contact that has a ρ_c in the range of $10^{-3} \Omega\text{-cm}^2$ to $10^{-6} \Omega\text{-cm}^2$ is considered an ohmic contact.

One means of reducing the ρ_c is to heavily dope the semiconductor which causes the barrier slope from Figure 1B to become steeper and W to be reduced. For values of W on the order of a few lattice spacings, electrons can quantum mechanically tunnel through the barrier when a voltage is applied and give rise to a current. The tunneling currents can be quite large and create a contact with a very low resistance. Ion implantation is used in the same manner.

The implantation reduces W and produces a contact with a low ρ_c .

A second method used to reduce the potential barrier is ion implantation. This is the method employed by this study. Ions are implanted into the semiconductor to increase the number of carriers in the material. An annealing process follows which activates the implanted ions by placing the ions in lattice sites. Consequently, both the implantation dosage and the annealing temperature affect the ρ_c .

Mathematical Development

By definition, the specific contact resistivity is given by

$$\rho_c = \left[\frac{dV}{dJ} \right]_{V \rightarrow 0}$$

where ρ_c = specific contact resistivity

V = voltage

J = current density

One of the methods of determining ρ_c is to use a transfer length measurement. In this method the actual measured quantity is the transfer length, L_T . L_T is the distance that the current has to flow under the contact before the fraction $(1 - \frac{1}{e})$ is transferred to the contact.

If a transfer length test pattern is used such as the one in Figure 2 and a current is passed between the end contacts, the potential developed can be measured against

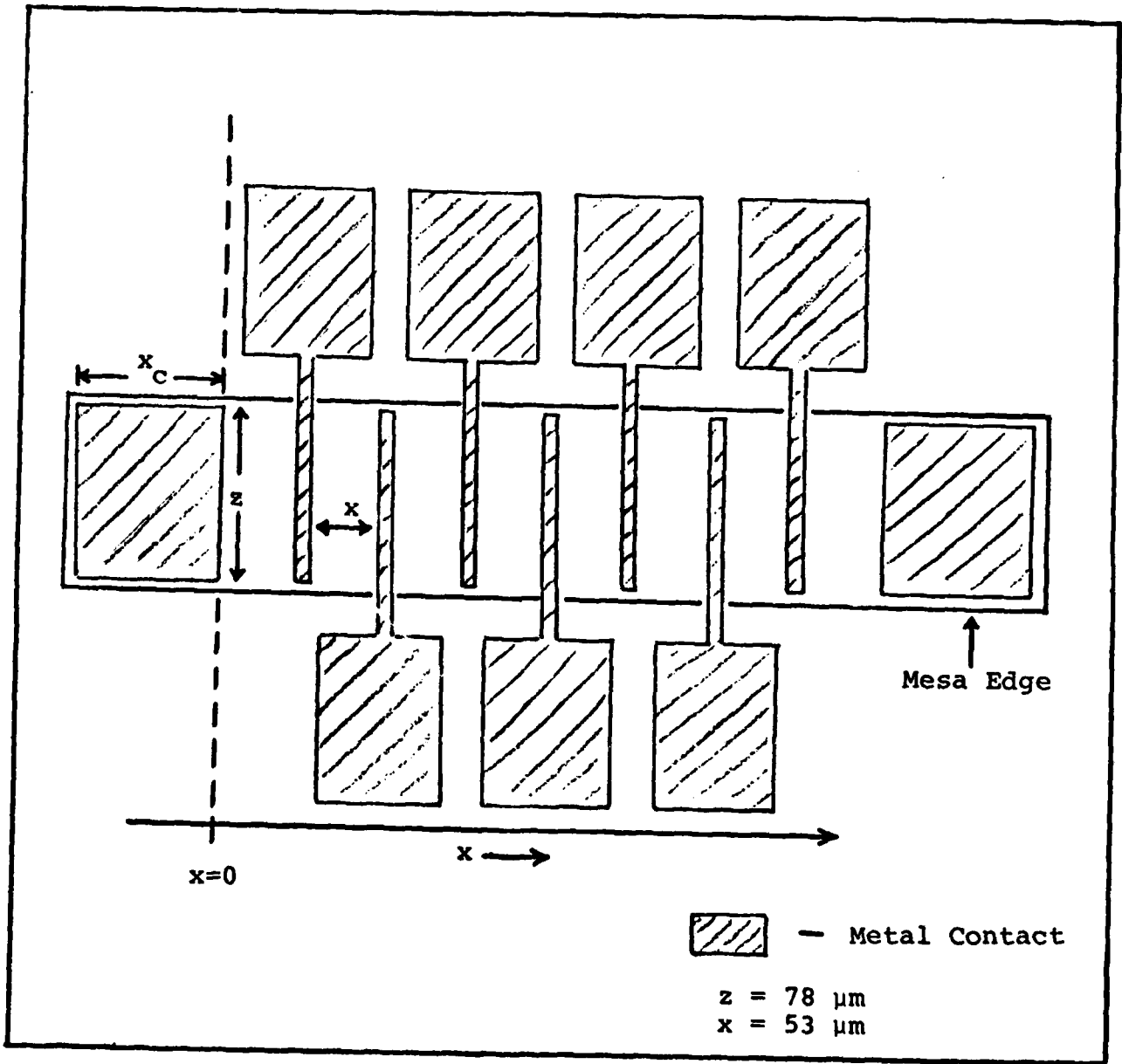


Figure 2. Transfer Length Pattern

the distance x . In the ideal case, the potential V_0 at $x=0$ should be zero, but in fact the potential V_0 at $x=0$ is not zero due to the contact resistance R_C and the resistance of the semiconductor active layer under the contact.

As the current passes through the conducting layer, a voltage drop $V(x)$ is due to the IR drop along the sheet resistance of the layer. Or

$$I = \frac{z}{R_{SH}} \frac{dV(x)}{dx}, \quad x > 0 \quad (3)$$

where z is the width of the contact. A plot of $V(x)$ versus x should give a straight line with a slope of $\left[\frac{IR_{SH}}{z} \right]$. R_{SH} is calculated from the slope since I and z are known.

Eq. (3) is valid as the current goes through the active layer. As the current reaches the contact some of it is lost to the contact because of ρ_C . Then the potential is given by

$$V(x) = V(0) \exp\left(-\frac{x}{L_T}\right), \quad x \leq 0. \quad (4)$$

From Eq. (4), L_T is defined as

$$L_T = \left(\frac{\rho_C}{R_{SH}} \right)^{1/2}$$

which can be also written as

$$\rho_C = R_{SH} L_T^2. \quad (5)$$

Experimentally, L_T is determined from the linear extrapolation of the line to $V=0$. R_C is given by

$$R_C = \frac{V(0)}{I}. \quad (6)$$

The previous equations were developed based on an assumption that the contact length is infinite. The contact is assumed to be infinitely long if L_T is much smaller than the contact length x_c . If the contact is not infinitely long then a more exact analysis must be performed. Wigen et al. (Ref 5) have done an explicit derivation of this case. The difference is the finite and infinite treatment lies in the boundary conditions used. In this treatment, Wigen proceeds as follows:

The current lost to the contact at any point λ is

$$dI(\lambda) = \frac{V(\lambda)}{\rho_c} z d\lambda . \quad (7)$$

All the current enters the contact, therefore I_{TOT} must go into the contact between $\lambda = x_c$ and $\lambda = 0$.

$$I_{TOT} = \int dI(\lambda) = \int_0^{x_c} \frac{V(\lambda)}{\rho_c} z d\lambda$$

and this gives the boundary condition on $V(\lambda)$.

If V_0 represents $V(\lambda=0)$, a constant, the voltage $V(\alpha)$ at any point $0 < \alpha < x_c$, is the sum of V_0 and the total $R_{SH} dI$ voltage drop up to that point.

$$V(\alpha) = V_0 + \int_0^\alpha dI(\lambda) \frac{R_{SH}}{z} (\alpha - \lambda) .$$

Substituting from Eq. (7), the above equation can be re-written as

$$V(\alpha) = V_0 + \int_0^\alpha \frac{V(\lambda)}{\rho_c} R_{SH} (\alpha - \lambda) d\lambda .$$

This equation must be solved to find $V(\lambda)$. Taking the derivative with respect to α , solving for $V(\alpha)$, and applying the boundary conditions results in

$$V(\alpha) = \frac{I_{TOT} \rho_C}{z L_T \sinh\left(\frac{x_C}{L_T}\right)} \cosh\left(\frac{\alpha}{L_T}\right).$$

Since $\alpha = x_C - x$, then

$$V(x) = \frac{I_{TOT} \rho_C}{z L_T \sinh\left(\frac{x_C}{L_T}\right)} \cosh\left(\frac{x_C - x}{L_T}\right) \quad (8)$$

which is a more exact expression for $V(x)$ than that given in Eq. (4). Eq. (8) simplifies to Eq. (4) in the case of an infinitely long contact where $L_T \ll x_C$.

When $x = 0$, Eq. (8) becomes

$$V(0) = \frac{I_{TOT} \rho_C}{z L_T} \frac{\cosh\left(\frac{x_C}{L_T}\right)}{\sinh\left(\frac{x_C}{L_T}\right)} \quad (9)$$

and when $V(x) = 0$,

$$x_{L_T} = L_T \frac{\cosh\left(\frac{x_C}{L_T}\right)}{\sinh\left(\frac{x_C}{L_T}\right)} \quad (10)$$

where x_{L_T} is the apparent transfer length. From Eq. (10), one can see the possibility of x_{L_T} being greater than x_C . In such a case

$$\rho_C = R_{SH} (x_{L_T})^2$$

would be in error. To solve for the correct expression for ρ_c , x_{L_T} and x_c are used to calculate the proper value of L_T .

Eq. (10) is rewritten as follows:

$$\frac{x_{L_T}}{x_c} = \frac{\cosh\left(\frac{x_c}{L_T}\right)}{\left(\frac{x_c}{L_T}\right) \sinh\left(\frac{x_c}{L_T}\right)} .$$

When $x_c/L_T \ll 1$, such as in the finite contact case, then

$$\cosh\left(\frac{x_c}{L_T}\right) \sim 1$$

and

$$\sinh\left(\frac{x_c}{L_T}\right) \approx \frac{x_c}{L_T} .$$

Substituting these expressions into Eq. (9), an expression for ρ_c is obtained

$$\rho_c = \frac{V(0)}{I_{TOT}} (z x_c) \quad (11)$$

Eq. (11) is valid when the contact cannot be considered infinite. A finite condition exists when ρ_c is large compared to R_{SH} , making the voltage drop in the contact due mostly to ρ_c . The contact may be taken as infinite if

$$\frac{x_c}{L_T} \geq 2 \quad (12)$$

or substituting in for L_T ,

$$x_c \left(\frac{R_{SH}}{\rho_c}\right)^{1/2} \geq 2 .$$

Determination of Specific Contact Resistivity

From the mathematical development, the approach to determine ρ_c becomes evident. A constant current is passed through two contacts and the potential created is measured against the distance x . A straight line can be plotted through the experimental points using a least squares technique. R_{SH} and R_c can be evaluated mathematically. L_T is extrapolated from data to evaluate ρ_c . If the contact satisfies the infinite condition

$$\frac{x_c}{L_T} \geq 2$$

then ρ_c is determined from

$$\rho_c = R_{SH} L_T^2 .$$

For an ohmic contact, the ρ_c should fall in the range of $10^{-3} - 10^{-6} \Omega\text{-cm}^2$. An ultra low specific contact resistivity is one that is less than $10^{-6} \Omega\text{-cm}^2$.

III Test Equipment and Sample Preparation

Prior to taking any measurements, the test equipment had to be assembled and the samples prepared. A brief description of the equipment is provided in this section, followed by the procedure used to fabricate the samples. Each step in the fabrication process is described and presented in the order performed.

Test Equipment

Figure 3 illustrates the basic equipment arrangement used for taking the required measurements. The equipment includes two probes that are used to pass a current through the contact pattern and an additional two probes which are used to detect the voltage drop between the two probe points. Each probe was mounted on a magnetic base and could be moved along three axes independently. Magnetic probe mounts secured the fine-tipped Osmium 15 probes to a probe station. A Keithley 616 Digital Electrometer was connected in series with a Keithley 225 current source. The resulting voltages were detected by a Keithley 6900 Digital Multimeter. To aid in placing the probes on the contact pattern, a Bausch and Lomb microscope with a 45x magnification was used. A light source illuminated the contact surface, but measurements had to be taken in a dark environment since the conducting layer

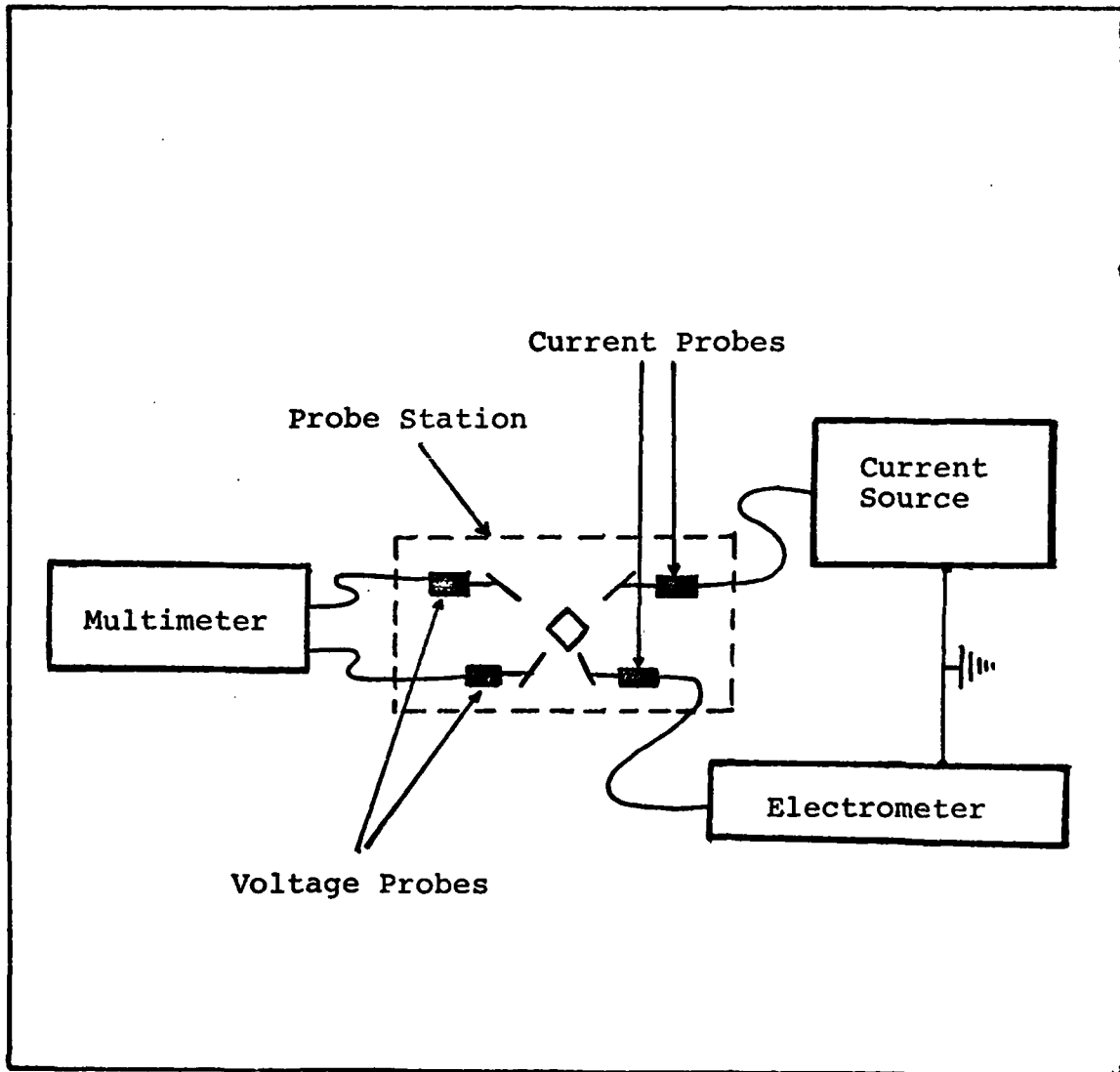


Figure 3. Schematic of Test Equipment

is optically sensitive. Thus when measurements were taken, the light source was turned off and a large black drop cloth was used to cover the entire probe station.

Sample Preparation

The experimental samples were fabricated from undoped GaAs substrates, Material Research, stock number A555/R. These substrates were found to be of fair quality. In order to prepare a sample for testing, the sample had to be cleaned, free-etched, implanted, pyrolytically capped, annealed, and mesa etched before the metal contact could be deposited and alloyed. Each of these steps will be covered in detail in this section.

Ion Implantation. The implantation dose was used as a parameter in this study. All samples were implanted with Si^{28} - ions of a fixed energy, 100 KeV, but were implanted at different doses. The doses used in this study were

$5 \times 10^{12} \text{ cm}^{-2}$	$1 \times 10^{14} \text{ cm}^{-2}$
$1 \times 10^{13} \text{ cm}^{-2}$	$3 \times 10^{14} \text{ cm}^{-2}$
$3 \times 10^{13} \text{ cm}^{-2}$	$1 \times 10^{15} \text{ cm}^{-2}$

and all samples were prepared under the supervision of Dr. Park.

Sample Cleaning. The cleaning of the sample is necessary prior to any further processing. First, the sample was washed and swabbed with basic-H solution, then rinsed with de-ionized (DI) water. Next it was subjected

to a chemical wash of trichloroethylene, acetone, and methanol, followed by a second rinse of DI water and blown dry with nitrogen.

Pyrolytic Encapsulation. The encapsulation of the implanted sample is necessary to prevent any losses of either dopants or host material atoms from the sample surface during annealing. All encapsulations were performed by Charlie Geesner of the Avionics Laboratory. Just prior to capping, the sample was soaked in HCl acid for one minute after which a layer of Si_3N_4 was deposited on the surface of the sample using a pyrolytic technique.

Annealing. The annealing was done in a furnace in an environment of flowing H_2 . For the purpose of this experiment, the annealing temperature was first fixed at 850°C for all doses, and then varied from $700^\circ - 900^\circ\text{C}$ for two fixed doses. A summary of the annealing temperatures and doses for the samples which were prepared is given in Table I. In general, the furnace was allowed to heat up to the desired temperature after which, the sample was placed in the furnace and was annealed for 15 minutes. Following the annealing time, the sample was cooled to 400°C before it was removed from the furnace.

Removal of Si_3N_4 Cap. Once the annealing process was completed, the Si_3N_4 cap was removed. The sample was soaked in HF for three to four minutes until the cap lifted off. Immediately afterwards, it was rinsed with DI water and blown dry.

TABLE I
Prepared Samples

Dose (cm^{-2})	Annealing Temperature			
	700°C	800°C	850°C	900°C
5×10^{12}			X	
1×10^{13}			X	
3×10^{13}	X	X	X	X
1×10^{14}			X	
3×10^{14}	X	X	X	X
1×10^{15}			X	

Mesa Etching. This process created a mesa region where the metal contact was deposited. It served to isolate the numerous contact patterns from current leakage. The etch must be deep enough to go beyond the depth of implantation, otherwise the applied-current path will seep around the contact pattern. If the current path is not perpendicular to the contact pattern, the mathematical analysis of the data fails.

The mesa etch process began with a voltage breakdown test of the surface. One expects a low breakdown since the surface should be highly conductive. The sample was cleaned in the same fashion as was described before. Next, the sample was baked-out at 200°C for 30 minutes in an N_2 ambient oven. The HMDS and AZ1470 photoresist (PR) were then applied

to the samples followed by a pre-bake at 70°C of 20 minutes.

Using a photographic mesa mask, the region to be etched off was exposed to ultraviolet light. Development takes 30 seconds in AZ351 developer. At this point, the exposed areas of the PR were lifted off so that the sample could be post-baked at 100°C for 30 minutes to harden the remaining PR. The actual etch was done with HF:H₂O₂:H₂O (1:1:8), which etches off about 100 Å per second. The samples were allowed to soak in the HF solution for one minute to etch off about 0.6 μm.

The remaining PR was removed with acetone after which a second voltage breakdown test was performed. This test was performed to determine the breakdown of the etched away portion of the sample, which should be a nonconducting surface. The breakdown voltage should be significantly increased as was the case for this work where the breakdown voltage went from 5V to 50V. Finally, the mesa step height was measured to check the etch depth.

Deposition of AuGe/Ni. At this point, the sample was finally ready for the deposition of the metal. The sample was cleaned and baked-out as previously described. The HMDS and PR were applied, and then the sample was baked at 70°C for 10 minutes. The contact pattern mask was aligned to the mesa and the sample was exposed to ultraviolet light. Following the exposure, the sample was soaked in chlorobenzene for 4.5 minutes and baked at 70°C for 15 minutes.

Development took 2 minutes and resulted in the removal of the PR where the contacts are desired. Immediately before deposition, the sample was soaked in dilute HF for five seconds to remove any oxidation on the surface. The actual deposition was done by technician Carol Travanski. The excess metal was lifted off by soaking the sample in acetone and using a gentle ultrasonic bath to shorten the soak time. The 2000 Å thick metal contact was composed of AuGe/Ni which consisted of 25% Ni and 75% AuGe, where 88% (by weight) of the AuGe is Au.

Alloying. The metal contact of AuGe/Ni must be alloyed to minimize the contact resistance. The usual alloying temperature varies from 400 to 450°C at different intervals of time, the higher the temperature, the shorter the time. In general, the lower temperature will produce the most uniform contact but not the lowest contact resistance. A higher alloying temperature results in a less uniform surface but a lower resistance, and too high of a temperature might cause a loss of As in the conducting surface. In this study, an alloying temperature of 450°C was used for 30 seconds.

The furnace was pre-heated to about 530°C after which the sample was pushed into the furnace. After approximately 2.5 minutes, the sample would reach 430°C and at this point the 30 second alloying time would begin. The sample was then partially pulled out of the furnace and allowed to cool to approximately 200°C before being removed completely.

Throughout the alloying process, the furnace was filled with flowing Ar gas.

An illustration of a finished sample with contacts is shown in Figure 4.

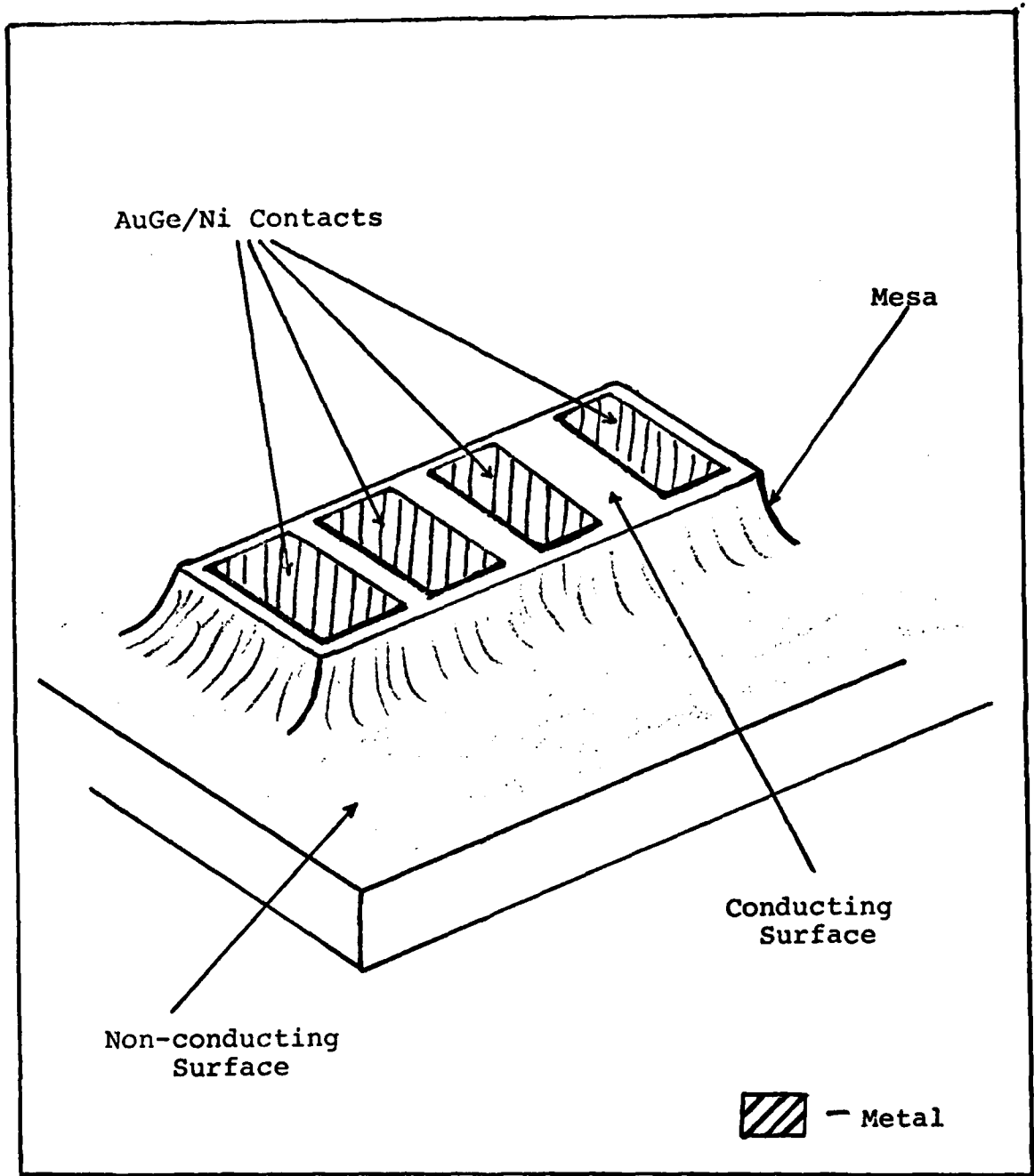


Figure 4. Illustration of Finished Sample with Contacts

IV Procedure

Two types of test patterns are commonly used to evaluate contact resistance, R_C , and contact resistivity, ρ_C . Both patterns follow the same theory and mathematical development. Any difference in the analysis of the data is noted in this section. Both patterns make use of the transfer length concept. However, in order to distinguish between the two designs, the patterns will be designated the ohmic contact pattern and the transfer length pattern. These were the names found in literature for the patterns. The geometry of each pattern is shown in Figure 5.

The ohmic contact pattern (Figure 5b) consists of seven rectangular metal contacts. Each pad is separated from the adjacent one by a different length: 3.39 μm , 8.67 μm , 13.69 μm , 18.91 μm , 23.99 μm , and 29.14 μm , respectively. The transfer length pattern (Figure 5a) has two large contact pads on the ends. Between the two pads are six equally spaced voltage pick-off strips. The ohmic pattern has a higher degree of accuracy while the transfer length pattern provides ease of measurement.

The procedure used to take measurements, calculate R_{SH} , R_C , L_T , and ρ_C , and compute the error bars will be presented in this section.

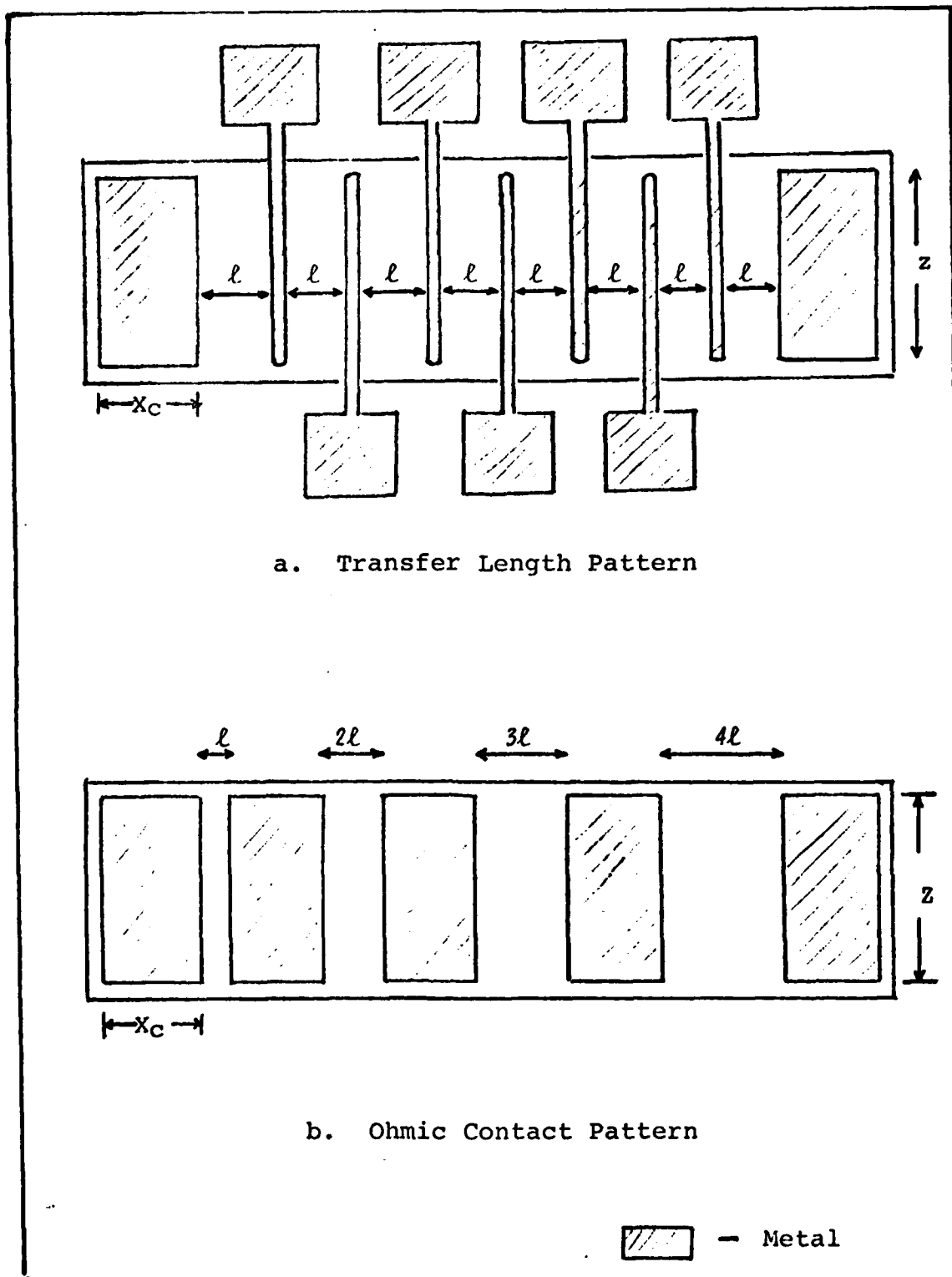


Figure 5. Test Pattern used to evaluate Specific Contact Resistivity

Measurements

Measurements are obtained by using a four-probe method. Before any measurements are taken a couple of checks must be made to ensure the contact is ohmic and the conductive surface is isolated. This section will describe how the checks and the measurements are made.

If the mesa etch is not deep enough, the applied current will diffuse around the mesa, therefore each pattern must be isolated to take proper measurements. In other words, only the mesa must contain the highly conductive surface. To check for current leakage, two patterns are selected that are positioned end to end. One current probe is placed on each pattern forcing the current to pass through an etched portion of the sample. By measuring the voltage drop between the patterns, one can determine if the etch region is still conductive or non-conductive. The resistance between patterns should be significantly higher than the resistance measured within a pattern. Often the current will be difficult to maintain between patterns, indicating good isolation.

All contacts must be ohmic. The traits of an ohmic contact are a linear relationship between the voltage and the current, and a non-preference to current polarity. To check for the linear relationship, merely send various currents through two contacts and note the respective voltage drops. Twice the current should have twice the

voltage drop. Non-preference to polarity means the absolute potential difference will not change as the current goes from positive to negative. This trait can be readily checked.

Once the pattern was confirmed as being isolated and the contact being ohmic, measurement of the contact resistance can begin. All measurements were taken using a four probe method. This method uses two current probes and two voltage probes. The advantage of this method compared to a two probe method is that the current probes' resistance is eliminated from the voltage readings.

When using the transfer length pattern, the current probes are placed on the large end pads. The current passes through the entire pattern and the current probes are never moved. One voltage probe is fixed on one of the end contact pads while the second voltage probe is moved from one finger contact to another.

Figure 6a illustrates the four probe method as it is applied to the transfer length pattern.

For the ohmic pattern, none of the probes are fixed. Current probes are set down on two adjacent pads and the voltage probes are positioned in a similar manner. The ohmic pattern always has a current probe and a voltage probe on a pad. Figure 6b shows the positioning of the probes on the ohmic pattern.

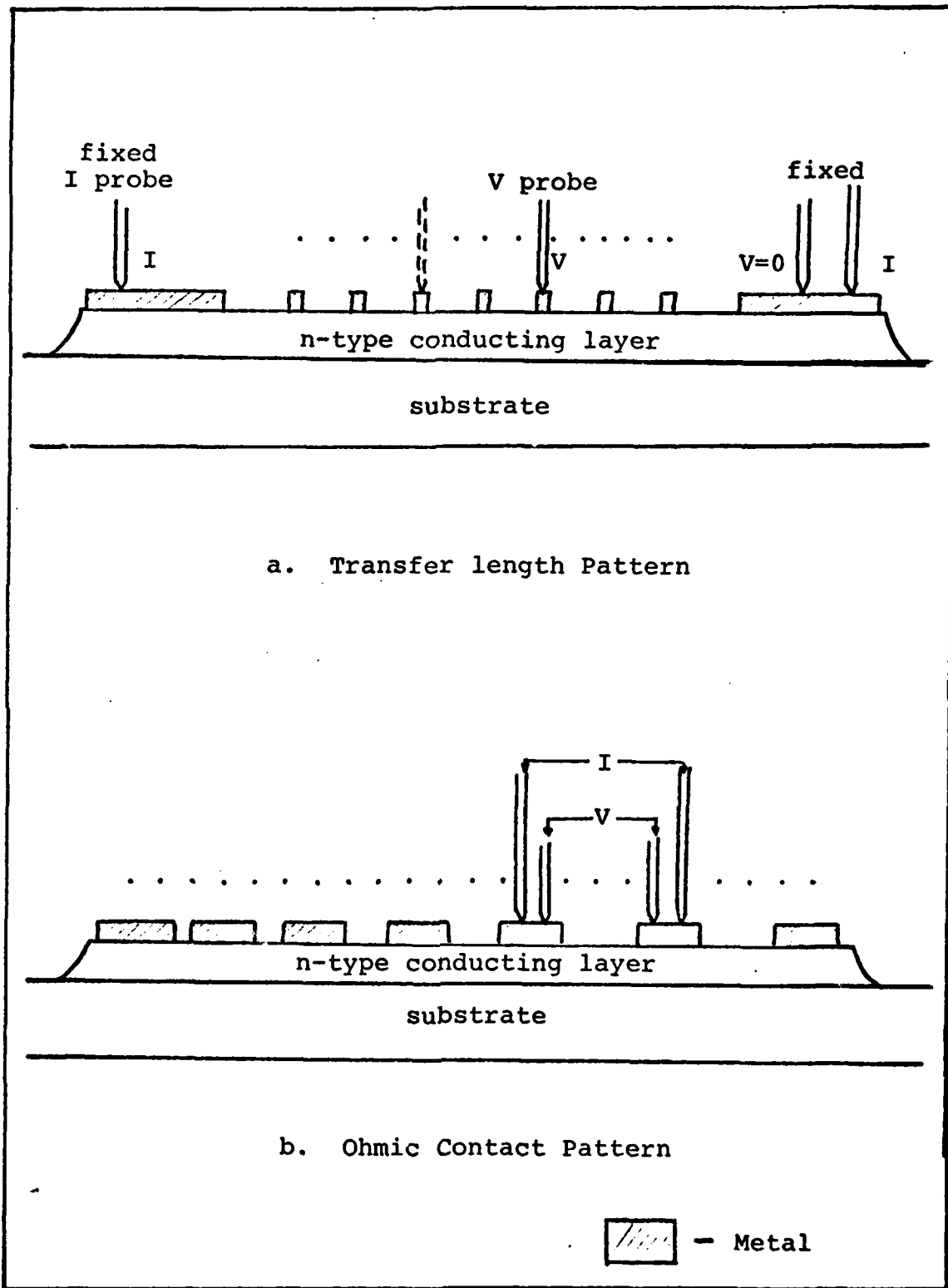


Figure 6. Probe Positions on Test Patterns

Calculations

For a given pattern, resistances are measured for various distances through the conductive material. The resistance is determined from Ohm's Law:

$$R = \frac{V}{I}$$

where R is the resistance, V is the voltage, and I is the current. The distance through the material, x, is the separation between contact points.

A plot of R versus x should yield a linear relationship. A non-linear relationship would suggest the contacts were not ohmic. The straight line can be plotted through the data points using a least square fit. Once a linear fit has been made to the points, the slope is easily determined. The sheet resistance, R_{SH} , is computed from

$$R_{SH} = z \cdot m$$

where z is the contact width (cm), and m is the slope of the line (Ω/cm).

The intercepts of the line give valuable information. The y-intercept is equal to twice the contact resistance, R_c , while the x-intercept is twice the transfer length, L_T . This statement is true for the ohmic contact pattern. Since the transfer length pattern is measured differently, $y(0)$ is equal to R_c , and $x(0)$ is equal to L_T . Regardless of which pattern is used, the slope remains the same.

Physically, the slope and R_C must be a positive value. The absolute value of the x-intercept is used for L_T . If the data should yield a negative y-intercept, then the results are invalid.

To compute ρ_C , the specific contact resistivity, one needs to know if the current sees an infinite or finite contact. A contact may be considered infinite if

$$x_C > 2 L_T$$

where x_C is the length of the contact. All measurements taken in this work met the above condition. Therefore, all the contacts could be considered electrically long or infinite.

If the y-intercept is positive and the contact is infinite, then ρ_C is computed from

$$\rho_C = R_{SH} L_T^2 .$$

Figure 7 depicts the expected graphical results from measurements using the two test patterns.

Error Bars

The error bars are computed from a statistical analysis of the data. On a given device, a large population of patterns are available. Close to 120 ohmic patterns and 60 transfer length patterns are on each device. A sample of the patterns are selected to represent the whole. Usually 9 - 12 patterns were measured on each wafer.

2

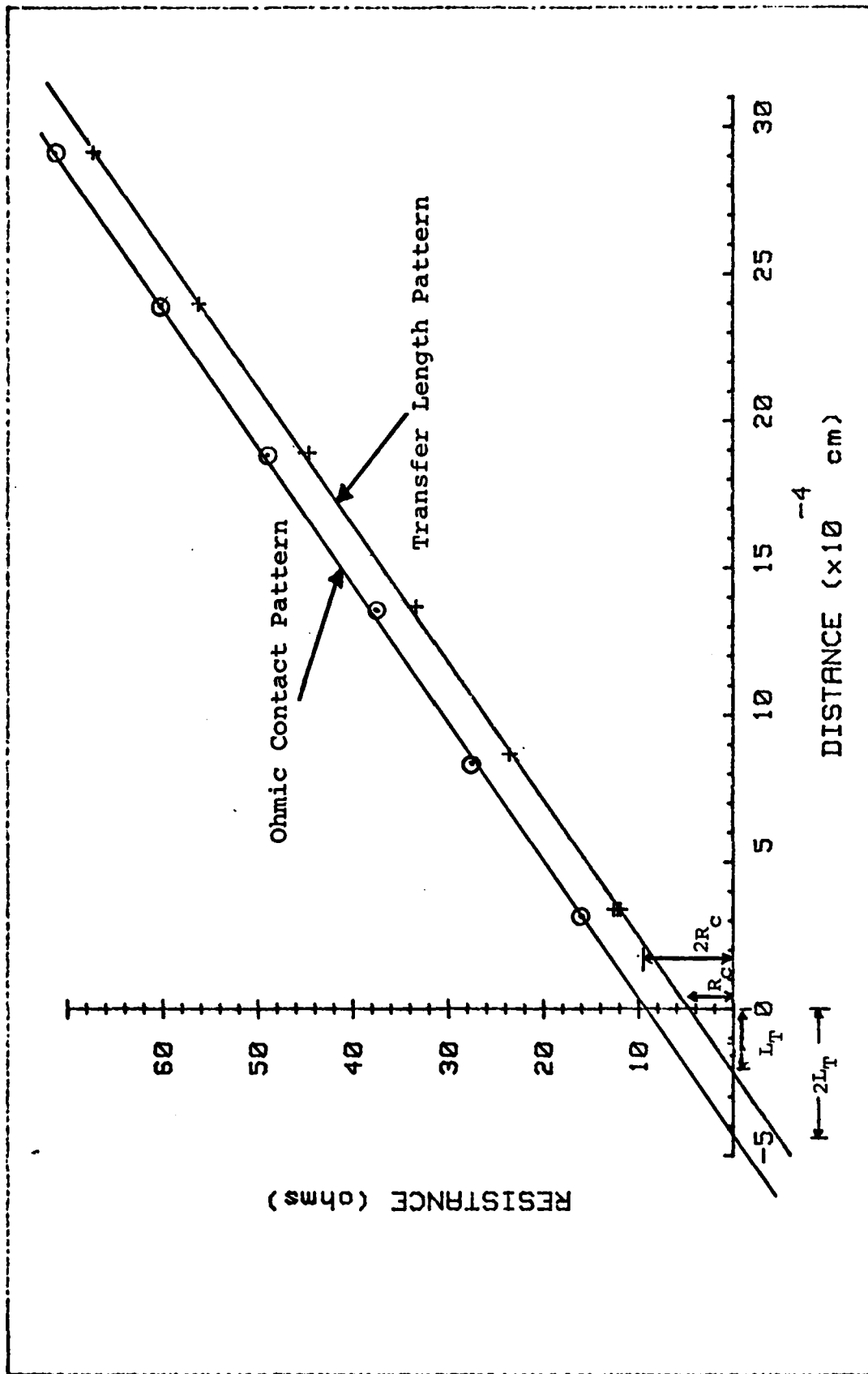


Figure 7. Expected Graphical Results

Statistically, the predicted range is derived from

$$\mu = \bar{x} \pm \frac{S_x}{\sqrt{n}} t \quad (13)$$

where \bar{x} is a mean value, S_x is the standard deviation, n is the number of measurements taken, and t is the degree of certainty for a given degree of freedom. All error bars shown in this study contain a 90% degree of certainty. In other words, the true value of the measurement has a 90% probability of falling within the range indicated by the error bars. t values were taken from a statistical chart (Ref 15: A-9).

V Results

All samples were checked for the electrical isolation of an individual pattern. This initial step confirmed the mesa etch was sufficiently deep. Next, each sample was tested for contact ohmicity. All the samples had ohmic contacts except one: the sample that was implanted to a dose of $5 \times 10^{12} \text{ cm}^{-2}$ and annealed at 850°C . Even after re-alloying, this sample did not form an ohmic contact. As a result, no data could be obtained from this sample. Following these initial tests, measurements could begin to be taken. Immediately two problems arose. Each sample had the two test patterns on it. A discrepancy developed between the findings of each pattern for the same sample. The two patterns were yielding values of ρ_c that were orders of magnitude apart. Secondly, when some of the data points were plotted out, the y-intercept would have a negative value. Clearly, a negative intercept indicates a negative contact resistance which is not physically possible. Both of these problems will be discussed further in this section, and the findings of this study will be presented.

Discrepancy Between Patterns

The two test patterns provide two ways to measure the same values. The question that needed to be answered was

which pattern gave the most reliable results? To determine this, Hall measurements were taken for samples implanted with three different doses, $1 \times 10^{13} \text{ cm}^{-2}$, $1 \times 10^{14} \text{ cm}^{-2}$, and $1 \times 10^{15} \text{ cm}^{-2}$, all annealed at 850°C . The Hall measurement provided very accurate values for the sheet resistivity, R_{SH} . Comparing the Hall value of R_{SH} to the values determined from the two patterns, one could gauge which pattern was yielding better results. The ohmic pattern consistently provided better measurements. The reason the transfer length pattern was inaccurate is still unclear.

The transfer length pattern measures voltage drops over a distance of $400 \mu\text{m}$, with the first data point at a distance of $53 \mu\text{m}$ and all other points $56 \mu\text{m}$ apart thereafter. The resistance across the total length varies from $1 - 1000 \Omega$, but the value of R_c to be determined is only about 2Ω . Therefore, the resolution near the y-intercept is poor and the R_c value is very sensitive to slight changes in the slope of the R versus distance curve. On the other hand, the ohmic pattern uses a maximum distance of $30 \mu\text{m}$ and produces resistances varying from $1 - 100 \Omega$. The ohmic pattern would seem to have a better resolution near the y-intercept because of the smaller range of the plot. In addition, the transfer length pattern has a y-intercept that is equivalent to R_c , while the ohmic pattern's y-intercept is equal to twice R_c . The ohmic pattern would probably yield a truer value of R_c . Based on the above discussion, the ohmic

pattern was selected for all further measurements and the transfer length pattern was abandoned.

Negative y-intercept

All measurements were taken from the ohmic pattern. However, the results were not always acceptable. Often the y-intercept would have a negative value which clearly indicated a flaw in the measurement or the evaluation. The pattern had been designed with spacings between the contact pads of 5 μm , 10 μm , 15 μm , 20 μm , 25 μm , and 30 μm . At closer inspection the spacings did not turn out to be increments of 5 μm . Photographs of the pattern were taken using a high-power microscope. The separations between pads were measured from the photograph with a high-grade meter ruler. The separations were found to be 3.39 μm , 8.67 μm , 13.69 μm , 18.91 μm , 23.99 μm , and 29.14 μm . These new x values significantly altered the plot. Virtually all measurements produced y-intercepts with positive values by using the new x values. Still, not all negative y-intercepts were eliminated.

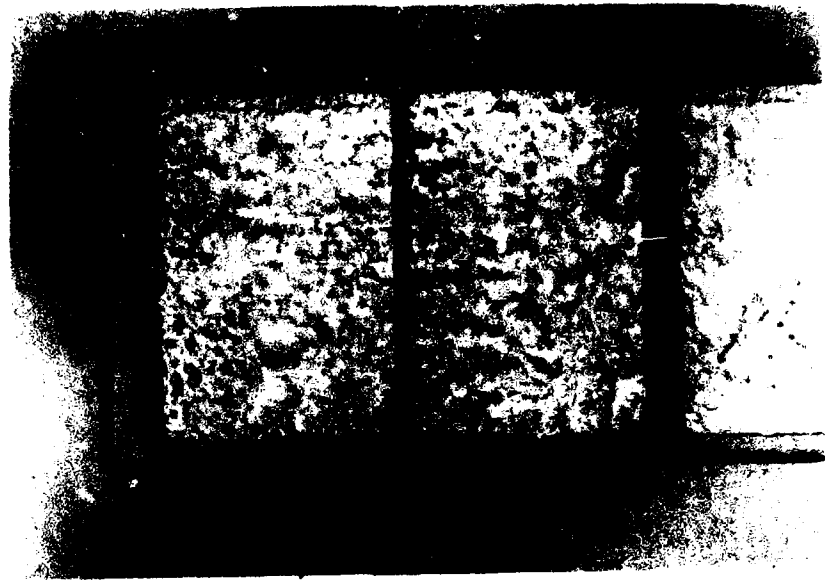
Once again, the failure of the measurements could be related to the contact pattern or difficulties of determining the correct R_c values due to the resolution problem. In the contact fabrication process, two masks are used: one to create the mesa and a second to pattern the contact design. The two masks must be manufactured so that the contacts lie directly on top of the mesa, however the two masks made for

this study were not perfectly aligned. The pictures taken of the contact pattern show how part of the metal contact lies off the mesa (see Figure 8). The misalignment would allow part of the current to flow around the contact instead of entirely perpendicular to the leading edge of the contact. Therefore, the contact/mesa misalignment would introduce some error in all measurements, although such an error would be slight.

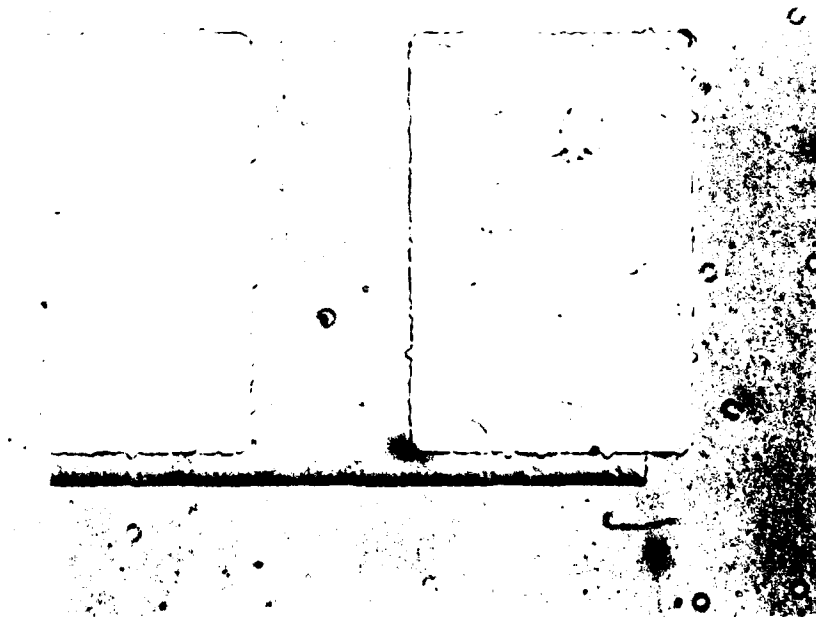
Findings

The experimental data when plotted formed a straight line. A typical plot of experimental data is given in Figure 9. For all plots the correlation coefficient was always better than 0.99. This would indicate that the bulk resistance or R_{SH} was behaving as it should and the ion implantation could be considered uniform over the dimensions of the pattern. Two variables were used in this study: the implantation dose and the annealing temperature.

Fixed Implantation Dose. Figure 10 is a plot of ρ_c versus annealing temperature for the two fixed ion doses. Although an exact value of ρ_c was difficult to determine because of questionable intercepts, this plot reveals that the annealing temperature over this range has virtually no effect on ρ_c . Nevertheless, the annealing temperature did alter the sheet resistance significantly. A plot of R_{SH} versus the annealing temperature is given in Figure 11.

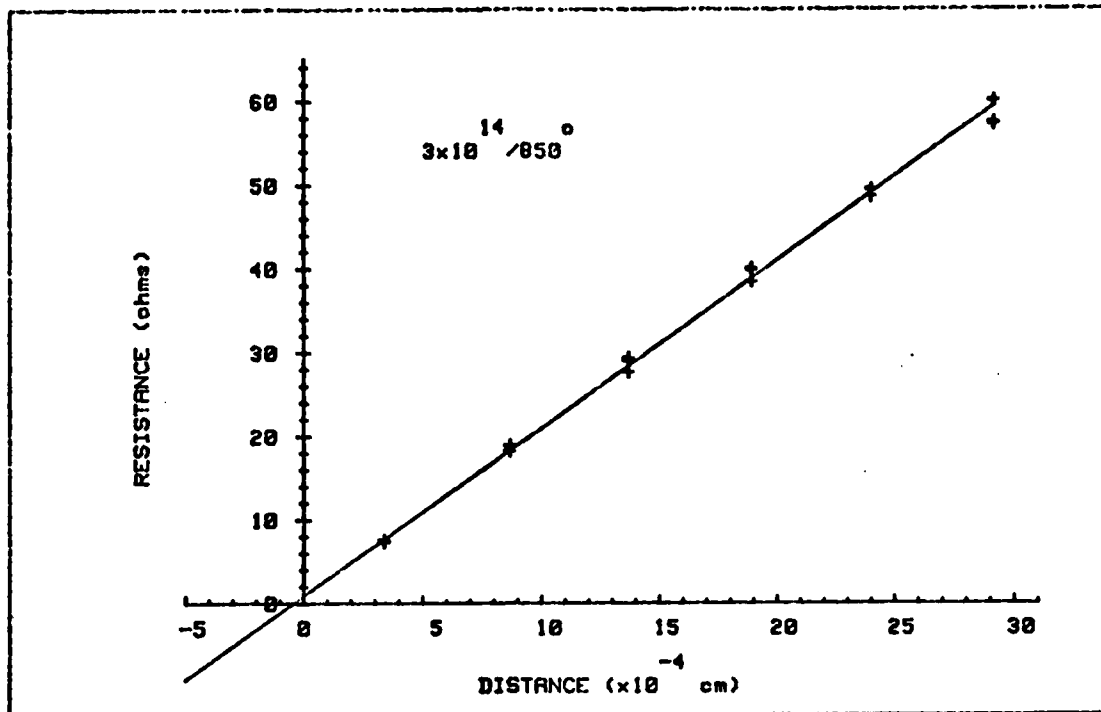


a. Contact Pads 1 and 2

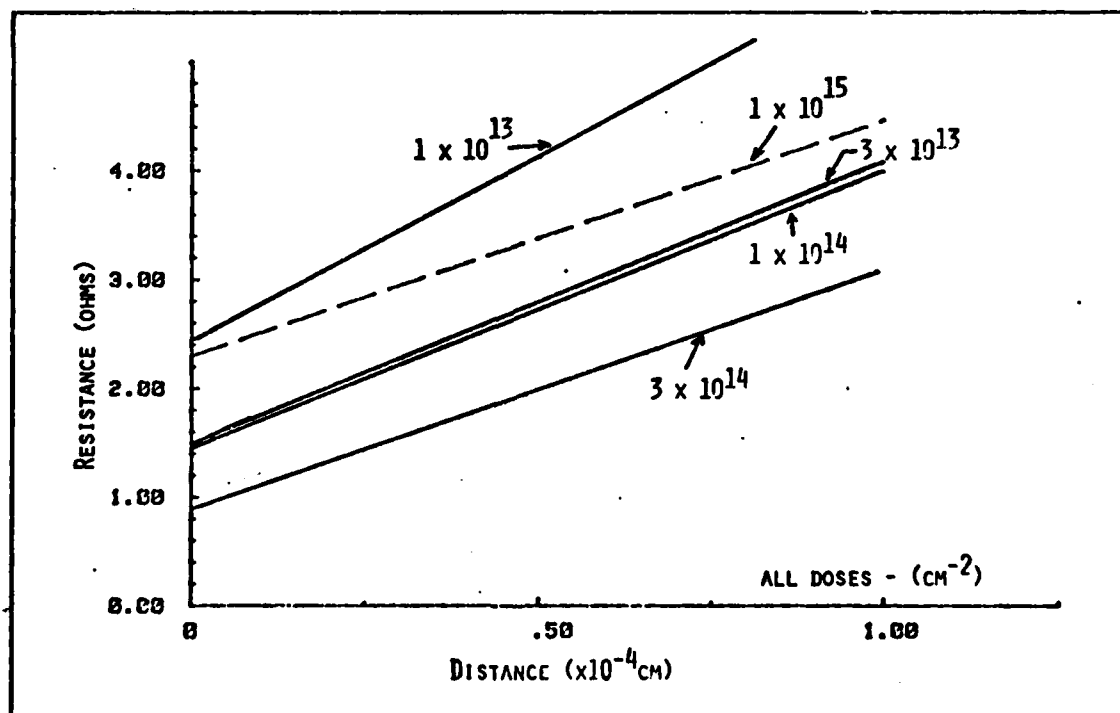


b. Contact Pads 6 and 7

Figure 8. Misalignment of Metal Contacts and Mesa



a. Plot of a single dose over entire range



b. y-intercept values of all doses

Figure 9. Resistance Versus Distance Plots of Experimental Data

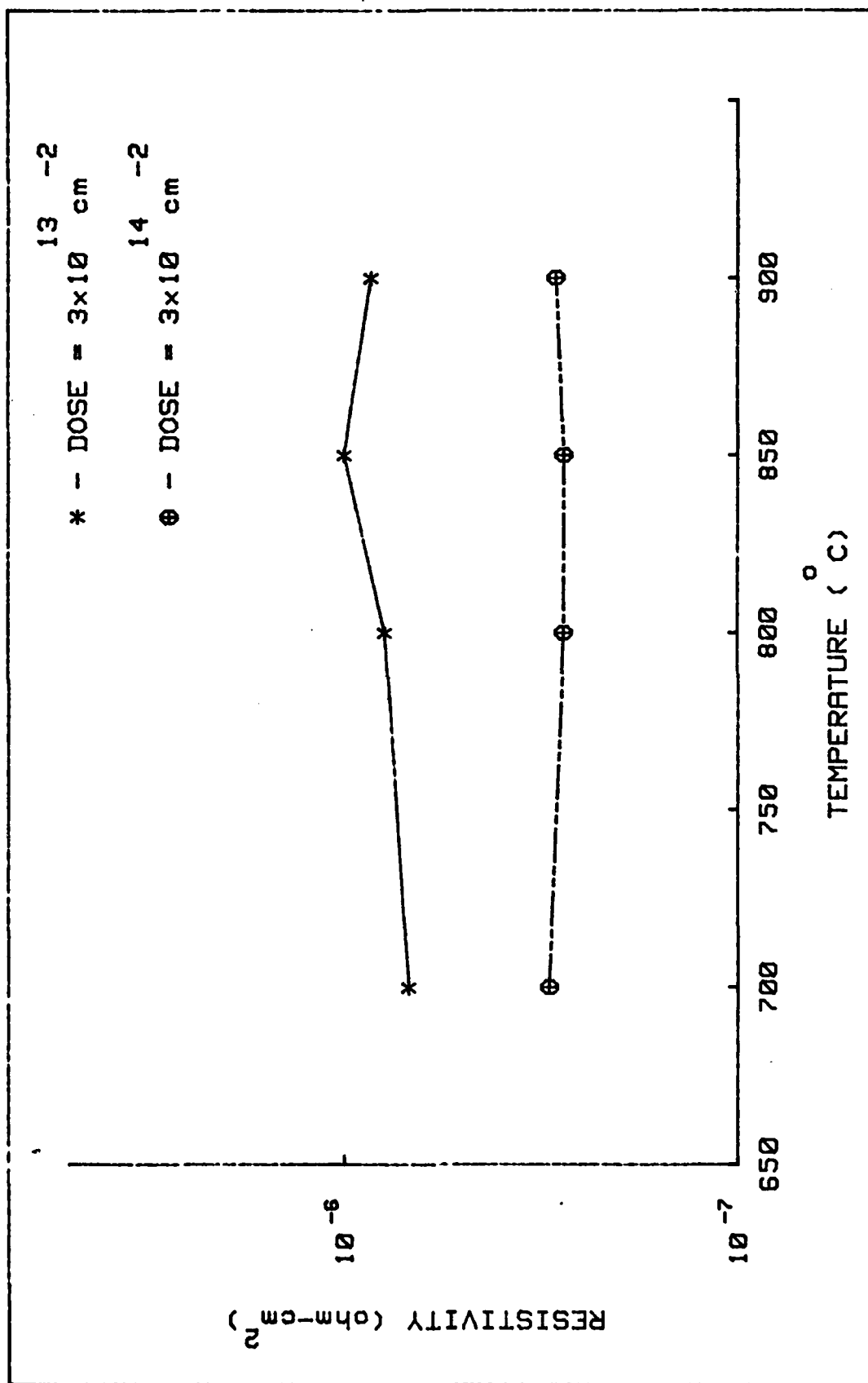


Figure 10. Plot of ρ_c vs - Annealing Temperature

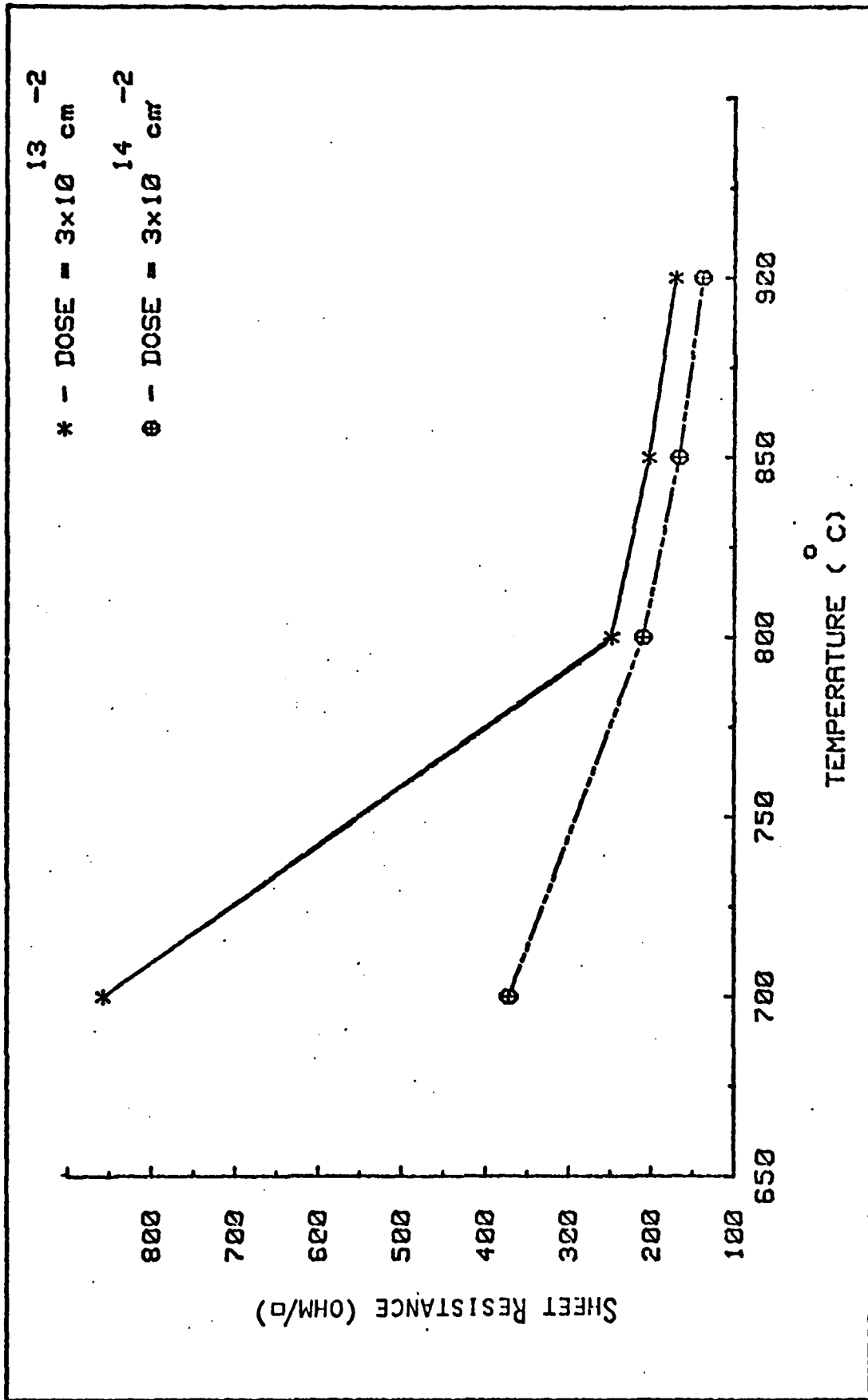


Figure 11. Plot of R_{SH} - vs - Annealing Temperature

This plot shows a definite decline in R_{SH} as the annealing temperature increases. The discrepancy between the annealing behavior of ρ_c and R_{SH} may also indicate that determining ρ_c values with considerable accuracy is a problem. However, ρ_c values for the dose of $3 \times 10^{14} \text{ cm}^{-2}$ is generally lower than those for the dose of $3 \times 10^{13} \text{ cm}^{-2}$ at all annealing temperatures.

Fixed Annealing Temperature. For this portion of the study, samples of various doses were annealed at 850°C for 15 minutes. Measurements were taken and a ρ_c was computed for each sample. A summary of the data obtained from the samples at a fixed annealing temperature is given in Table II.

Resistivity is calculated from the relation

$$\rho_c = R_{SH} L_T^2$$

where R_{SH} is taken from the slope of the plot. R_{SH} measurements were quite consistent for all data taken from one sample. The calculated R_{SH} was compared to the R_{SH} value determined by Hall measurement. The comparison of the Hall R_{SH} and the experimentally derived R_{SH} values is given in Figure 12. This plot shows that the experimental values are in good agreement with the Hall measurements.

While the R_{SH} values were very consistent for different measurements on the same sample, the same could not be said about the L_T values. L_T is determined by the x-intercept. Often the x-intercept would vary by a factor of two or three.

TABLE II

Data Summary - Fixed Annealing Temperature

Dose (cm^{-2})	$\frac{\text{HALL}}{R_{\text{SH}}}$ (Ω/\square)	R_{SH} (Ω/\square)	R_{C} (Ω)	L_{T} ($\times 10^{-5} \text{cm}$)	ρ_{C} ($\times 10^{-7} \Omega\text{-cm}^2$)
1×10^{13}	249.71	256.16	2.44	7.33	14.3
3×10^{13}	---	196.13	1.50	5.80	9.99
1×10^{14}	188.75	191.90	1.46	5.82	6.57
3×10^{14}	---	166.47	.895	4.10	2.78
1×10^{15}	155.10	164.13	2.30	10.6	18.8

Since L_{T} drives the equation used to compute ρ_{C} , ρ_{C} values are very sensitive to slight variations in L_{T} .

Figure 13 is a plot of ρ_{C} versus dose. The points shown use the mean value of ρ_{C} for that dose. The error bars represent the range in which the true value for ρ_{C} could be found (90% certainty). The sample with the lowest ρ_{C} value was the sample implanted at $3 \times 10^{14} \text{ cm}^{-2}$. In general, the greater the dose, the lower the ρ_{C} , until the dose of $3 \times 10^{14} \text{ cm}^{-2}$ is reached. At that point, the trend reverses itself and ρ_{C} increases with the dose.

The reasons that ρ_{C} increases for the dose of $1 \times 10^{15} \text{ cm}^{-2}$ are not well understood at present. Although the implanted dose is very high, the sheet carrier concentration and R_{SH} are not substantially improved from the values given for the $3 \times 10^{14} \text{ cm}^{-2}$ dose. This implies that significant

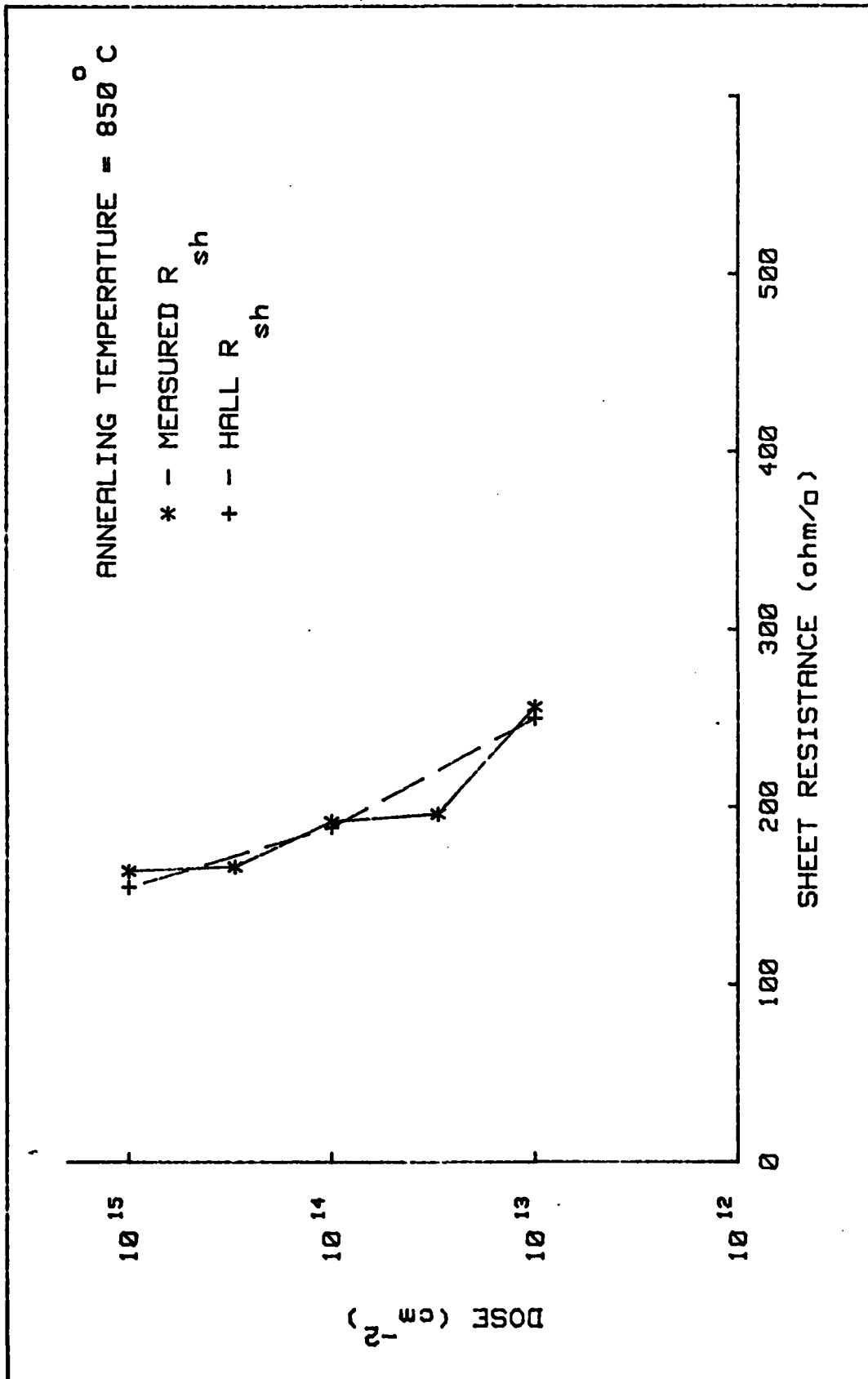


Figure 12. Plot of Dose-vs- R_{SH}

b

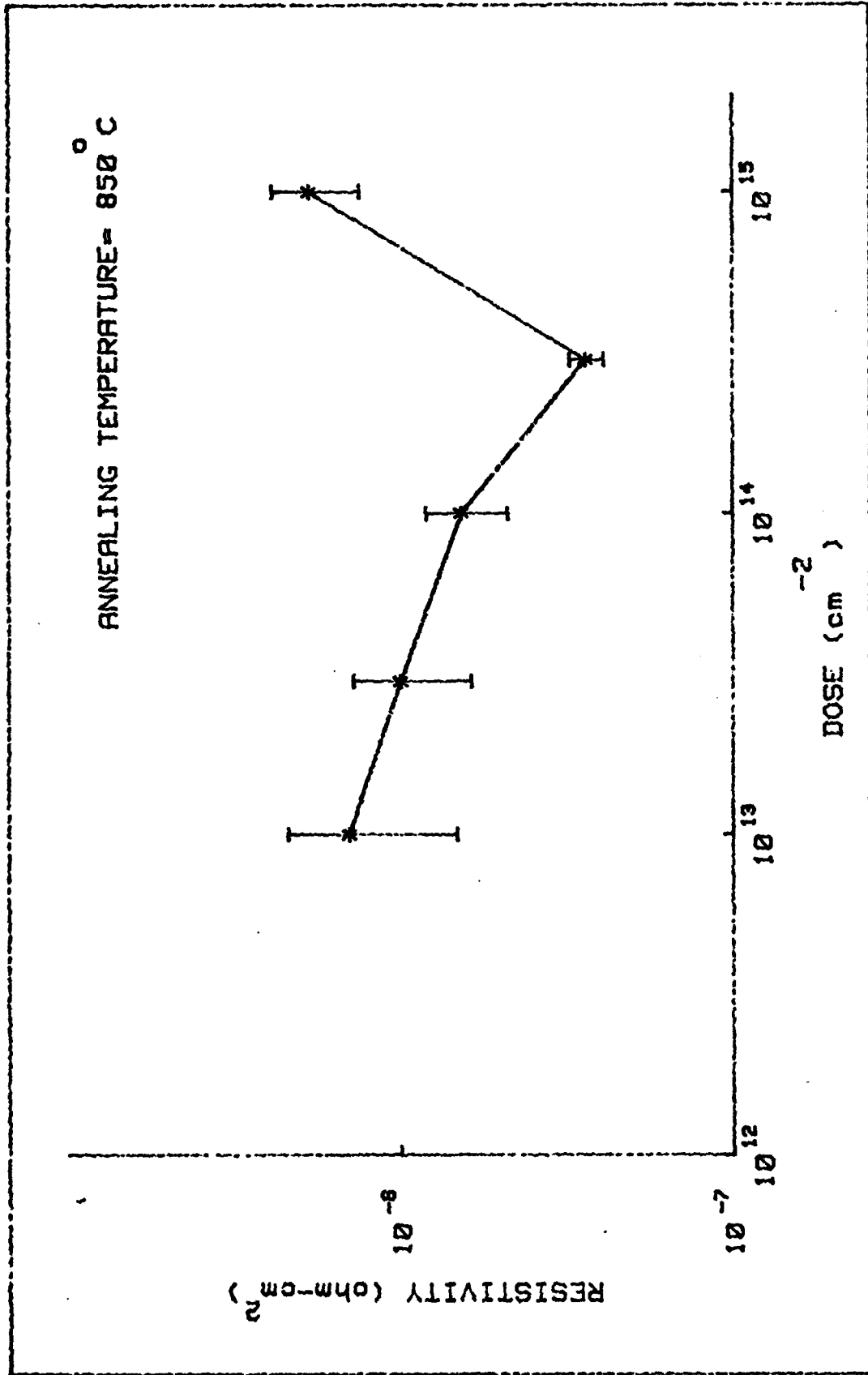


Figure 13. Plot of ρ_c vs - Dose

implantation damage may have remained for this sample, and therefore ρ_c is higher than that for the dose of $3 \times 10^{14} \text{ cm}^{-2}$.

Based on the findings of this work, the following trends were observed. If the dose is fixed and the annealing temperature is varied, no real change in ρ_c occurs. However, a definite change in R_{SH} is observed: as the annealing temperature is increased the sheet resistance decreases. When the annealing temperature is fixed and dose is varied, then a change in ρ_c is easily seen. As the dose increases, the resistivity decreases until the minimum ρ_c is reached at the dose of $3 \times 10^{14} \text{ cm}^{-2}$, after which ρ_c increases rapidly with the dose. The minimum value of ρ_c that was obtained is $2.8 \times 10^{-7} \Omega - \text{cm}^{-2}$.

VI Recommendations/Conclusions

From the outset, this study sought to investigate the effect of the ion implantation dose and the annealing temperature on the specific contact resistivity. With the dose held constant, the annealing temperature was varied over a range of temperatures and ρ_c was computed. While ρ_c did not change with the variations in annealing temperature, a change was noted in the R_{SH} values. R_{SH} decreased as the annealing temperature increased. The discrepancy in the annealing behavior of ρ_c and R_{SH} may indicate that ρ_c is not being determined accurately. However, the ρ_c values for the dose of $3 \times 10^{14} \text{ cm}^{-2}$ were lower than those of the $3 \times 10^{13} \text{ cm}^{-2}$ dose. When the annealing temperature was fixed at 850°C and the dose was varied, a more definite trend was observed. In general the greater the dose, the lower the ρ_c until the minimum ρ_c was reached at a dose of $3 \times 10^{14} \text{ cm}^{-2}$, after which an increase in dose produced a sharp increase in ρ_c . This higher ρ_c found in higher doses could be due to greater ion implantation damage. The minimum ρ_c value obtained was $2.78 \times 10^{-7} \Omega\text{-cm}^2$ for a dose of $3 \times 10^{14} \text{ cm}^{-2}$ annealed at 850°C .

While the findings were useful, the experimental insight gained proved to be the most beneficial result of this work. These measurements had not been attempted before at

the Avionics Laboratory and unrefined experimental procedures contributed to inaccuracies in measurements. Recommendations for improving measurement accuracy are presented in the remainder of this section.

The shortcomings of this work are directly related to the contact test pattern dimension. The inability to obtain accurate intercept values from the plot of experimental data was caused by the relatively large dimensions of the pattern.

A higher degree of accuracy could be obtained if the test pattern would be re-designed. The contact pattern shown in Figure 14 has been proposed by Dr. A. Ezis. In the proposed pattern the contacts are separated 2 μm , 3 μm , 4 μm , 6 μm , and 8 μm . Given that

$$z = 70 \mu\text{m}$$

$$x_c = 60 \mu\text{m}$$

$$\text{Dose} = 3 \times 10^{14} \text{ cm}^{-2}$$

$$\rho_c = 1 \times 10^{-7} \Omega \text{ cm}^2$$

one can calculate the expected values of the intercepts.

From Figure 12, one can get

$$R_{SH} \cong 170 \Omega/\square$$

so therefore

$$\text{Slope} = \frac{R_{SH}}{z} = 2.43 \Omega/\mu\text{m}$$

and

$$L_T = \left(\frac{\rho_c}{R_{SH}} \right)^{1/2} = .243 \mu\text{m}$$

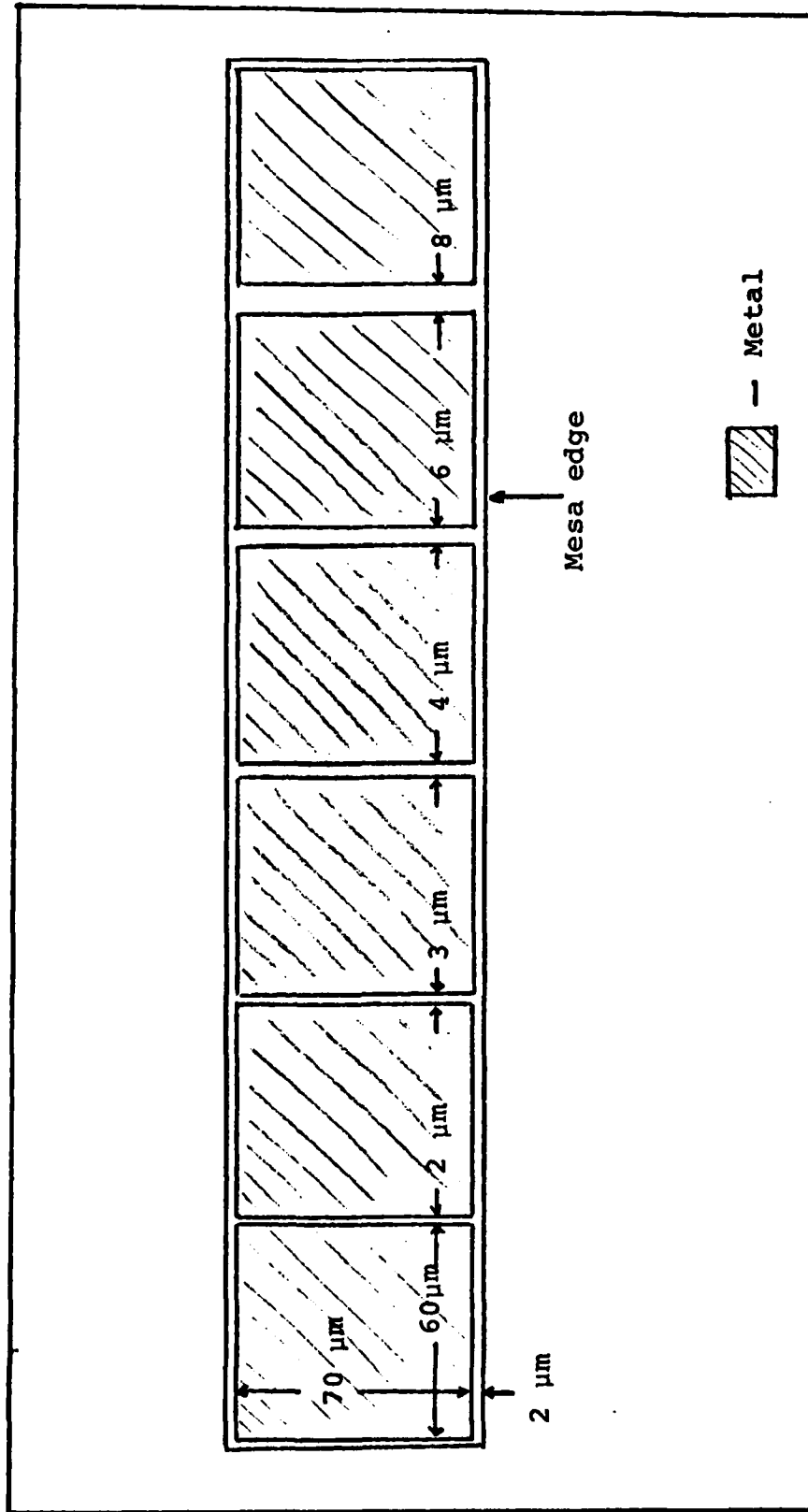


Figure 14. Proposed Ohmic Contact Test Pattern

from which one obtains

$$R_C = (\text{Slope}) L_T = .59 \Omega .$$

The proposed pattern does satisfy the infinite condition:

$$x_C > 2 L_T$$

since

$$60 \mu\text{m} > .5 \mu\text{m} .$$

For the proposed pattern dimensions the resistance measurements would range from 0 to 20 Ω as x goes from 0 to 10 μm . The y -intercept, which is $2 R_C$, would be -1.2Ω . The x -intercept, which is $2 L_T$, would be $\sim .5\mu\text{m}$. These intercept values should be easily determined by the proposed pattern since the scale of the plot is greatly reduced.

Further improvements in this study could also be implemented. The semiconductor substrate was of fair quality. Upgrading the quality of the substrate could improve the consistency of the measurements. The slightly inferior substrate could have contributed to experimental variations in the data.

When the new mask is manufactured for the proposed contact pattern, care needs to be taken to design a mesa mask that is aligned to the pattern. Alignment eliminates the concern of current flowing other than perpendicular to the contact interface.

Lastly, the optics in the probe station needs to be of a greater magnification. The greater magnification is needed to see the contact pads and the separation between pads. The optics could be improved by simply replacing the eyepieces with lenses of 20x or better.

The recommendations suggested in this section should provide more reliable results. The frequency of questionable intercepts should be reduced if not eliminated and a greater degree of precision in ρ_c measurements could be achieved. The measurement method described in this work is a simple experimental means of determining R_{SH} , R_c , L_T and ρ_c . With the modifications given in this section, the measurements could be quite accurate and the results easily reproduced.

Bibliography

1. Yu, A. Y. C. "Electron Tunneling and Contact Resistance of Metal-Silicon Contact Barriers," Solid State Electronics, 13: 239-247 (1970).
2. Berger, H. H. "Contact Resistance and Contact Resistivity," Journal of Electrochemical Society: Solid State Science and Technology, 119; 507-514 (April 1972).
3. Inada, Taroh, and Shigeki Kato. "Ohmic Contacts on Ion Implanted n-Type GaAs Layers," Journal of Applied Physics, 50(6): 4466-4468 (June 1979).
4. Ohata, Keiichi, Tadatoshi Nozaki, and Nobuo Kawamura. "Improved Noise Performance of GaAs MESFET's with Selectivity Ion-Implanted n+ Source Regions," IEEE Transactions on Electron Devices, Ed-24(8): 1129-1130 (August 1977).
5. Wigen, Philip E., Marlin O. Thurston, Electron Device Contact Studies. AFWAL-TR-81-1294. Wright-Patterson AFB, Ohio: Avionics Laboratory, May 1982.
6. Berger, H. H. "Models for Contacts to Planar Devices," Solid States Electronics, 15(3): 145-158 (1972).
7. Schuldt, S. B. "An Exact Derivation of Contact Resistance to Planar Devices," Solid States Electronics, 21: 715-719 (1978).
8. Mott, N. F. Proc. Camb. Phil. Soc., 34; 568 (1938).
9. Schottky, W. Naturwiss, 26; 843 (1938).
10. Cox, R. H. and Strack, H. "Ohmic Contacts for GaAs Devices," Solid State Electronics, 10; 1213 (1967).
11. Eckhardt, G. "Overview of Ohmic Contact Formation on N-type GaAs by Laser and Beam Annealing," Laser and Electron Beam Processing Materials. New York: Academic Press, (1980).
12. Ehret, J. E., Y. K. Yeo, K. K. Bajaj, E. T. Rodine, G. Das, Characterization of Ion Implanted Semiconductors. AFWAL-TR-80-1171. Wright-Patterson AFB, Ohio: Avionics Laboratory, November 1980.

13. Singh, Hausila P. "D. C. Properties of Passivated GaAs MESFETS." Report for the Wright-Patterson AFB Aeronautical Laboratories. September 1981.
14. McKelvey, John P. Solid State and Semiconductor Physics. New York, Harper and Row, 1966, pp. 478-498.
15. ----- . Calculator Decision-Making Sourcebook. Product Supplementary Book. Texas Instrument Incorporated, 1977.
16. Beyer, William H. CRC Standard Mathematical Tables (25th Edition). Boca Raton, Florida: CRC Press Inc., 1978, pp. 509-510.
17. Brophy, James J. Basic Electronics for Scientists (3rd Edition). New York: McGraw-Hill Book Company, 1977, pp. 2-4, 123-155.
18. Chang, I. F. "Contact Resistance in Diffused Resistors," Journal of Electrochemical Society: Solid State Science, 117; 368-372 (March 1970).
19. Hower, D., Hooper, S., Cairno, K., Fairman, C., and Tremere, J. R. Metals and Semiconductors, New York, McGraw-Hill, 1975, pp. 178-181.
20. Kwok, S. P., M. Feng, Victor Eu. "Characterization of Ultra Low Ohmic Contact Resistance."
21. Yeo, Y. K. "Contact Resistivity," notes. Wright-Patterson AFB Avionics Laboratory, April 1982.
22. Yeo, Y. K. "Determination of the Specific Contact Resistance," notes. Wright-Patterson AFB Avionics Laboratory, August 1982.
23. Yeo, Y. K. "Hall-Effect/Sheet Resistivity (Van der Pauw Method)," notes. Wright-Patterson AFB Avionics Laboratory, January 1978.

Vita

Diane M. Fischer was born 22 February 1959 in Peru, Indiana, the daughter of Curtis H. and Mary Fischer. After graduation in 1977 from Zweibrücken American High School, Zweibrücken, Germany, she attended Angelo State University, San Angelo, Texas. In May 1981 she was graduated with honors with the degree of Bachelor of Science in Physics. After receiving her commission as Lieutenant in the USAF, she entered active duty in May 1981. Her first military assignment was to the Air Force Institute of Technology in the Graduate Engineering Physics curriculum.

Permanent address: 7971 Hanford Way
Sacramento, California

This thesis was typed by Mrs. Diane Katterheinrich

UNCLASSIFIED

SECURITY CLASSIFICATION OF THIS PAGE (When Data Entered)

REPORT DOCUMENTATION PAGE		READ INSTRUCTIONS BEFORE COMPLETING FORM
1. REPORT NUMBER AFIT/GEP/PH/82D-8	2. GOVT ACCESSION NO. A124 689	3. RECIPIENT'S CATALOG NUMBER
4. TITLE (and Subtitle) STUDY OF OHMIC CONTACTS ON Si ²⁸ - IMPLANTED GaAs		5. TYPE OF REPORT & PERIOD COVERED MS Thesis
		6. PERFORMING ORG. REPORT NUMBER
7. AUTHOR(s) Diane M. Fischer 2Lt, USAF		8. CONTRACT OR GRANT NUMBER(s)
9. PERFORMING ORGANIZATION NAME AND ADDRESS		10. PROGRAM ELEMENT, PROJECT, TASK AREA & WORK UNIT NUMBERS
11. CONTROLLING OFFICE NAME AND ADDRESS		12. REPORT DATE December 1982
		13. NUMBER OF PAGES 61
14. MONITORING AGENCY NAME & ADDRESS (if different from Controlling Office)		15. SECURITY CLASS. (of this report) UNCLASSIFIED
		15a. DECLASSIFICATION/DOWNGRADING SCHEDULE
16. DISTRIBUTION STATEMENT (of this Report) Approved for Public Release; Distribution Unlimited		
17. DISTRIBUTION STATEMENT (of the abstract entered in Block 20, if different from Report)		
18. SUPPLEMENTARY NOTES Approved for public release: LAW AFR 130-17. <i>Lynn E. Volmer</i> LYNN E. VOLMER Dean for Personnel and Professional Development Air Force Institute of Technology Wright-Patterson AFB, Ohio 45433 19 JAN 1983		
19. KEY WORDS (Continue on reverse side if necessary and identify by block number) Gallium Arsenide Low Resistance Contact Ion Implantation Specific Contact Resistivity Silicon Implanted GaAs Resistivity Ohmic Contact AuGe/Ni Ohmic Contacts		
20. ABSTRACT (Continue on reverse side if necessary and identify by block number) A study of fabricating a low resistant contact on Si ²⁸ - implanted n-type GaAs was conducted. Ion doses of $1 \times 10^{13} \text{ cm}^{-2}$ to $1 \times 10^{15} \text{ cm}^{-2}$ and annealing temperatures of 700°C to 900°C were tested in order to achieve the lowest specific contact resistivity. Experimental results show that a low specific contact resistivity of $2.78 \times 10^{-7} \Omega\text{-cm}^2$ can be obtained on GaAs layers which have been formed by Si ²⁸ ($3 \times 10^{14} \text{ cm}^{-2}$) implantation in undoped semi-		

DD FORM 1473
1 JAN 73

EDITION OF 1 NOV 65 IS OBSOLETE

UNCLASSIFIED

SECURITY CLASSIFICATION OF THIS PAGE (When Data Entered)

UNCLASSIFIED

SECURITY CLASSIFICATION OF THIS PAGE(When Data Entered)

(continued)

19. Transfer Length
Annealing Temperature
Transmission Line

(continued)

20. insulating GaAs annealed at 850°C using an oxygen-free chemical vapor deposited Si_3N_4 layer as an encapsulant followed by subsequent deposition of AuGe/Ni ohmic contacts. Recommendations are discussed concerning further studies and a design for a new contact test pattern which would improve the degree of accuracy of resistivity measurements.

UNCLASSIFIED

SECURITY CLASSIFICATION OF THIS PAGE(When Data Entered)